Neurobiology of Aging 64 (2018) 123–138

Contents lists available at ScienceDirect

Neurobiology of Aging

journal homepage: www.elsevier.com/locate/neuaging

Genome-wide circulating microRNA expression profiling reveals potential biomarkers for amyotrophic lateral sclerosis

José Manuel Matamala [a,b,c,d], Raul Arias-Carrasco [d], Carolina Sanchez [d], Markus Uhrig [d], Leslie Bargsted [a,b,f], Soledad Matus [a,f,g], Vinicius Maracaja-Coutinho [d], Sebastian Abarzua [e], Brigitte van Zundert [e], Renato Verdugo [c], Patricio Manque [d,*], Claudio Hetz [a,b,f,h,i,**]

[a] Biomedical Neuroscience Institute (BNI), Faculty of Medicine, University of Chile, Santiago, Chile
[b] Program of Cellular and Molecular Biology, Institute of Biomedical Sciences, University of Chile, Santiago, Chile
[c] Department of Neurological Sciences, Faculty of Medicine, University of Chile, Santiago, Chile
[d] Center for Genomics and Bioinformatics, Faculty of Sciences, Universidad Mayor, Santiago, Chile
[e] Center for Biomedical Research, Faculty of Biological Sciences and Faculty of Medicine, Universidad Andres Bello, Santiago, Chile
[f] Center for Geroscience, Brain Health and Metabolism (GERO), Santiago, Chile
[g] Neurounion Biomedical Foundation, Santiago, Chile
[h] Buck Institute for Research on Aging, Novato, CA, USA
[i] Harvard School of Public Health, Boston, MA, USA

ARTICLE INFO

Article history:
Received 11 August 2017
Received in revised form 18 December 2017
Accepted 21 December 2017
Available online 29 December 2017

Keywords:
Amyotrophic lateral sclerosis
MicroRNAs
Biomarkers
miR-142-3p
miR-1249-3p

ABSTRACT

The occurrence of mutations of *TDP-43*, *FUS*, and *C9ORF72* in amyotrophic lateral sclerosis (ALS) suggests pathogenic alterations to RNA metabolism and specifically to microRNA (miRNA) biology. Moreover, several ALS-related proteins impact stress granule dynamics affecting miRNA biogenesis and cellular miRNA levels. miRNAs are present in different biological fluids and have been proposed as potential biomarkers. Here we used next-generation sequencing to perform a comparative analysis of the expression profile of circulating miRNAs in the serum of 2 mutant superoxide dismutase 1 transgenic mice. Top hit candidates were then validated using quantitative real-time polymerase chain reaction, confirming significant changes for 6 miRNAs. In addition, one of these miRNAs was also altered in mutant TDP-43 mice. Then, we tested this set of miRNAs in the serum from sporadic ALS patients, observing a significant deregulation of hsa-miR-142-3p and hsa-miR-1249-3p. A negative correlation between the revised ALS functional rating scale and hsa-miR-142-3p levels was found. Bioinformatics analysis of the regulatory network governed by hsa-miR-142-3p identified TDP-43 and C9orf72 as possible targets, suggesting a connection with ALS pathogenesis. This study identifies miRNAs that are altered in ALS that may serve as potentials biomarkers.

1. Introduction

Amyotrophic lateral sclerosis (ALS) is a progressive fatal neurodegenerative disease involving the degeneration of motor neurons in the spinal cord, brainstem, and cerebral cortex (Kiernan et al., 2011; Peters et al., 2015). The vast majority of ALS cases are considered sporadic (sALS) and only 5%–10% have a family history (fALS) (Leblond et al., 2014). Despite the clinical heterogeneity, median survival of ALS remains on 3 years, with 10% of the patients surviving over 8 years (Al-Chalabi et al., 2016). Currently the diagnostic criteria mainly rely on the identification of concurrent upper motor neuron and lower motor neuron dysfunctions, disease progression, and the exclusion of other pathologies (de Carvalho et al., 2008; Turner et al., 2013a,b). However, the application of these criteria excludes around 40% of recent onset ALS cases from recruitment in clinical trials (Traynor et al., 2000). In addition, several studies described an average of 14 months of delayed diagnosis (Chiò, 1999; Nzwalo et al., 2014), increasing the risk of losing a possible therapeutic window (Sreedharan and Brown, 2013; Turner et al., 2009). Thus, there is an urgent need to

* Corresponding author at: Center for Genomics and Bioinformatics, Universidad Mayor, Camino la Piramide 5730, Santiago, Chile. Tel.: +56 223281414.
** Corresponding author at: Institute of Biomedical Sciences, Sector B, second floor, Faculty of Medicine, University of Chile, Independencia 1027, Santiago 70086, Chile. Tel.: +56 229786506.
E-mail addresses: patricio.manque@umayor.cl (P. Manque), chetz@med.uchile.cl, chetz@hsph.harvard.edu (C. Hetz).
URL: http://www.hetzlab.cl

0197-4580/$ – see front matter © 2017 Elsevier Inc. All rights reserved.
https://doi.org/10.1016/j.neurobiolaging.2017.12.020

identify biomarkers to improve diagnosis, to monitor disease progression, and to develop effective disease-modifying treatments (Lesko and Atkinson, 2001; Bowser et al., 2011; Turner et al., 2009).

Repeat expansion in the intronic region of *C9ORF72* gene and mutations in the gene encoding cytosolic superoxide dismutase 1 (*SOD1*) are the most frequent genetic causes of fALS, accounting for around 70% of fALS cases, whereas mutations in TAR DNA-binding protein (also known as TDP-43) and fused in sarcoma/translated in liposarcoma (*FUS/TLS*) genes represent nearly 10% of the fALS cases (Renton et al., 2014). Although the etiology of ALS remains poorly understood, altered proteostasis (Hetz and Mollereau, 2014) and mRNA metabolism (Sreedharan and Brown, 2013) are common features of the disease process. For example, misfolded TDP-43 is the main component of ubiquitin-positive inclusions in sALS and fALS patients (Neumann et al., 2006). TDP-43 localizes predominantly to the nucleus, where it regulates several aspects of RNA processing and metabolism (Janssens and Van Broeckhoven, 2013). In ALS, TDP-43 is misplaced in the cytosol where it is hyperphosphorylated and forms insoluble ubiquitin-positive aggregates (Neumann et al., 2006). TDP-43 was identified as part of nuclear Drosha and cytoplasmic Dicer complexes, crucial ribonucleoproteins implicated in microRNA (miRNA) biogenesis (Buratti et al., 2010; Polymenidou et al., 2011). Importantly, repeat expansions in the intronic region of *C9ORF72* are also associated with nucleocytoplasmic transport (Freibaum et al., 2015). Similarly, alteration in other ALS-related genes has been linked to disturbances on RNA metabolism (Paez-Colasante et al., 2015). Together, all this evidence has led to the hypothesis of a pathogenic role of altered RNA metabolism in ALS (Freischmidt et al., 2013; Sreedharan and Brown, 2013).

In addition to modified mRNA homeostasis, many ALS-related genes have been reported to disrupt miRNA metabolism (Emde et al., 2015; Kawahara and Mieda-Sato, 2012). miRNAs are small noncoding RNAs (sncRNAs) with a key role in controlling gene expression via RNA-dependent post-transcriptional silencing mechanisms (Bartel, 2009). Importantly, miRNAs are regulated under stress conditions, reflecting the activation of pathogenic pathways. For example, mutant SOD1, C9ORF72, TDP-43, and FUS impact stress granule dynamics, affect miRNAs biogenesis, and therefore reduce cellular miRNA levels (Emde et al., 2015; Gal et al., 2016; Medinas et al., 2017; Taylor et al., 2016). Studies in many neurodegenerative diseases, including Alzheimer's and Parkinson's diseases, have revealed a specific pattern of miRNA deregulation, suggesting a direct involvement in the disease process (Abe and Bonini, 2013; Shioya et al., 2010).

miRNAs can be detected not only in tissues but also in different biological fluids including the serum and plasma showing high stability (Arroyo et al., 2011). Monitoring the precise pattern or fingerprint of circulating miRNAs has proven useful as potential biomarkers of different diseases, due to their high specificity (Freischmidt et al., 2015; Gilad et al., 2008; Schöler et al., 2010; Turner et al., 2009, 2013a,b). In the context of ALS, miRNAs exhibit an aberrant expression profile in central nervous system (CNS) tissues from transgenic mouse models and patients with sALS and fALS (Campos-Melo et al., 2013; Koval et al., 2013). At mechanistic level, studies in mutant SOD1 transgenic mice suggest a functional contribution of miRNAs to disease progression (Gupta et al., 2012; Koval et al., 2013; Parisi et al., 2016; Williams et al., 2009; van Zundert and Brown, 2016). Altogether, these findings support a pathogenic role of miRNA dysregulation in ALS, independent of the etiology of the disease.

Various studies have shown a deregulation of peripheral miRNAs levels (serum and blood cells) in ALS patients (Benigni et al., 2016; De Felice et al., 2012, 2014; Freischmidt et al., 2013, 2015; Takahashi et al., 2015). However, there is a high discrepancy in the identified miRNAs among studies, probably associated to the variability of phenotypes among ALS patients, differences in sample processing, quantification methods, and detection thresholds. Although a single miRNA may not be sufficient to unambiguously diagnose ALS, fingerprinting a cluster of miRNAs together with clinical data would probably increase the reliability of a correct and early diagnosis. Such a panel of ALS-specific miRNAs could serve as a signature that mirrors disease progression and might help monitoring the evolution of the disease and its modification with therapeutic interventions in clinical trials (Turner and Talbot, 2013).

Here, we defined the global pattern of serum circulating miRNAs derived from 2 genetically independent ALS mouse models during late presymptomatic and symptomatic stages to identify transversal and conserved biomarkers. Candidate miRNAs were then monitored on a cohort of sALS patients identifying 2 potential disease biomarkers. Remarkably, one of them, hsa-miR-142-3p, was predicted to target the expression of TDP-43 and C9orf72. The potential use of these miRNAs for complementing clinical diagnosis and disease evolution is discussed.

2. Materials and methods

2.1. Transgenic mouse models

All animal experiments were performed in 3 ALS transgenic mouse models: $SOD1^{G86R}$, $SOD1^{G93A}$, and $TDP43^{A315T}$. For $SOD1^{G86R}$ and $SOD1^{G93A}$ experiments, we defined 3 disease stages for our biochemical analysis: (1) early presymptomatic stage, aged 60 days (P60); (2) late presymptomatic stage, aged 90 days (P90); and (3) symptomatic stage, which is defined as the time when signs of motor-related problems and/or symptoms occurred. The mean age of the appearance of disease signs defined in the models was 162.4 ± 24.7 days and 139.6 ± 11.8 days for $SOD1^{G86R}$ and $SOD1^{G93A}$ transgenic mice, respectively. The experiments in $TDP43^{A315T}$ transgenic mice were performed only during the symptomatic stage of the disease (mean age of 71.1 ± 9.5 days). Animals were maintained under a 12:12-hour light/dark cycles with free access to food and water.

$SOD1^{G86R}$ transgenic mice express a mouse transgene equivalent to the human gene mutation Gly85Arg encoding a SOD1 enzyme with low enzymatic activity (stock number Jackson's laboratory 005110) (Matus et al., 2013). The advantage of this model is that the endogenous SOD1 promoter drives the expression of the mutant SOD1 gene with low overexpression levels. This model was obtained from Jackson's laboratory in a FVB background, but it was moved to a C57BL/6 background.

$SOD1^{G93A}$ mice express the human SOD1 cDNA (Gurney et al., 1994). This high copy number mutant SOD1 transgenic model has a B6SJL mixed genetic background (stock number Jackson's laboratory 002726). These 2 SOD1 transgenic mice develop a disease resembling ALS characterized by muscle atrophy and limb paralysis at 4–5 months of age and early death.

$TDP43^{A315T}$ transgenic mice express a mutated version of TDP-43 protein under the control of the mouse prion protein promoter, developing a progressive and fatal neurodegenerative disease (Wegorzewska et al., 2009). This model was originally published with a C57BL/6 CBA–mixed genetic background, but the mouse colony used was obtained on a C57BL/6 genetic background (stock number Jackson's laboratory 010700) (Esmaeili et al., 2013; Wegorzewska et al., 2009). To avoid intestinal problems, these animals are fed with jellified food (Herdewyn et al., 2014).

For all the animals, the onset of symptomatic disease stage was determined by a loss of 5% in total body weight and visual inspection of disease signs (Castillo et al., 2013; Nassif et al., 2014). The researcher was not blind to the genotype of the mice included in the experiments and measurements represent standard assays in

the laboratory performed by several researchers. In brief, we monitored and scored the appearance of abnormal limb clasping, tremor felt in hind limbs, dirty appearance of the skin, backbone arching, and paralysis. We assigned to each visual observation a score 1 when the symptom appeared, 3 when it increased, or 5 when the phenotype was severe. As the backbone arching and paralysis frequently appear as a result of a severe neuronal dysfunction, the score for these symptoms started from 3 instead of 1. Using this score, disease onset was defined as the moment when the value reached more than 10. The end stage of the disease was determined as the time when an animal was not able to right itself up within 30 seconds after being placed on its back. All animal experiments were performed according to procedures approved by the "Guide for the Care and Use of Laboratory Animals" published by the U.S. National Institutes of Health (NIH Publication, 8th Edition, 2011). The animal care and experimental protocols were approved by the Bioethical Committee of the Faculty of Medicine, University of Chile.

2.2. ALS patients

A total of 27 patients, 13 men and 14 women, were evaluated with suspected diagnosis of ALS. Each patient was interviewed according to a standardized clinical questionnaire and underwent a neuromuscular clinical examination. Electrophysiological evaluation (nerve conduction studies and needle electromyography) was performed only in those patients who did not take the previously mentioned test or for which the diagnosis was uncertain. Patients with ALS were clinically staged using the revised ALS functional rating (ALSFRS-R) scale (Cedarbaum et al., 1999), and muscle strength was tested using the Medical Research Council rating scale (Medical Research Council, 1976). The disease progression rate (PR) was calculated for each patient (PR = [48 − current ALSFRS-R score]/disease duration in months at recruitment), allowing classification of the clinical progression into 3 stages: fast PR (PR: >1), medium PR (PR: 0.5–1), and slow PR (PR: <0.5) (Kimura et al., 2006).

With the goal to study circulating miRNAs as the serum biomarker for ALS, we defined the following criteria: (a) inclusion criteria: (1) patients aged over 18 years with definite or probable ALS according to the Awaji criteria (de Carvalho et al., 2008); (2) patients who are still able to give consent to participate voluntarily in the study. (b) Exclusion criteria: (1) acute inflammatory or infectious diseases defined by the presence of one or more of the following criteria: fever (>37.5 °C) or hypothermia (<35 °C), tachypnea (>20 breaths per minute), tachycardia (>90 beats per minute), leukocytosis (>12,000 mm^3) or leukopenia (<4000 mm^3) or left shift (immature neutrophil count in peripheral blood >10%), and C-reactive protein >10 mg/dL; (2) history of chronic inflammatory or autoimmune disease; (3) impaired renal function, defined by glomerular filtration rate <30 mL/min as calculated by the Cockroft-Galt (GFR = [140 − age] × weight/creatinine × 72); (4) history of diabetes mellitus and/or fasting plasma glucose >125 mg/dL; (5) history of chronic liver damage or liver failure defined by prothrombin time <60% and/or total bilirubin >3.0 mg/dL; (6) oncologic pathology; and (7) patient with tracheostomy or users of noninvasive mechanical ventilation.

All ALS patients and healthy controls underwent general blood examinations to rule out significant systemic diseases, including blood count, C-reactive protein, prothrombin time, partial thromboplastin time, creatinine, plasma electrolytes, glucose, total bilirubin, alanine transaminase, aspartate aminotransferase, gamma-glutamyl transpeptidase, and serum creatine kinase (CK).

Of the 27 patients initially evaluated, 7 met exclusion criteria. Therefore, 20 ALS patients were finally included in the study. We also included 20 healthy controls, with age and sex exactly matched to the ALS patients, recruited from staff and relatives of patients attending the Service of Neurology, Hospital del Salvador (Santiago, Chile). Recruitment, screening, and enrollment of patients and controls and all clinical studies were conducted at the Service of Neurology, Hospital del Salvador. The study was approved by the ethics committee of the Hospital del Salvador and University of Chile. All patients and healthy controls provided written informed consent before participation. All methods followed the provisions of the Declaration of Helsinki and were carried out in accordance with relevant guidelines and regulations (STROBE Statement).

2.3. Blood sample collection

Blood samples were taken from $SOD1^{G86R}$ and $SOD1^{G93A}$ transgenic mice and nontransgenic (Non-Tg) littermate control animals during 3 disease-related stages: (1) early presymptomatic stage; (2) late presymptomatic stage; and (3) during the symptomatic stage. From the $TDP43^{A315T}$ transgenic mice, blood samples were obtained only during the symptomatic stage of the disease. Mice were anesthetized using 100/10 mg/kg ketamine/xylazine by intraperitoneal injection. Once anesthetized, the blood was collected by intracardiac puncture by a percutaneous technique using a 25G needle diameter. The whole blood was collected in HemogardTM tubes (BD Vacutainer).

Blood samples were obtained from human patients and controls by venous puncture. About 2 mL of blood samples were taken from each ALS patient and healthy control. The whole blood was collected in HemogardTM tubes (BD Vacutainer).

Separation of the serum, from murine and human blood samples, was carried out by centrifugation at 3000 × g for 10 minutes. The supernatant was collected and centrifuged again at 2600 × g for 10 minutes to remove cellular debris. Then, the supernatant serum was stored at −80 °C and was not thawed until use. Hemolytic serum was excluded from further analysis.

2.4. RNA extraction

For next-generation sequencing (NGS), RNA was extracted from pooled serum samples from late presymptomatic (n = 5 animals) and symptomatic (n = 5 animals) $SOD1^{G86R}$ and $SOD1^{G93A}$ transgenic mice and from their respective Non-Tg littermate control mice (n = 5 animals). For the quantitative reverse transcription polymerase chain reaction (qRT-PCR) analysis, RNA was extracted from individual serum samples, taken from the same mice selected for the NGS study (Fig. 1). The same RNA extraction protocol was carried out for serum samples collected from mice and humans. In summary, total RNA was isolated from 400 μL of serum (from pooled or individual serum samples) using Trizol LS reagent (Invitrogen, Carlsbad, CA) in combination with miRNeasy Serum/Plasma Kit (Qiagen, Germany) as previously described (Zhong et al., 2008). For normalization of sample-to-sample variation, a spiking in control was used: 25 fmol of synthetic *C. elegans* miRNA cel-miR-39 (Qiagen, Germany) was added to each sample during the extraction protocol. RNA was dissolved in 12 μL of RNase-free water and then stored at −80 °C until analysis. The total RNA concentration was determined using RiboGreen RNA Quantitation Kit (Invitrogen). RNA profile was determined using RNA 6000 Pico Kit by a 2100 Bioanalyzer (both Agilent Technologies).

2.5. cDNA library preparation and NGS

The samples were sequenced using an Illumina MiSeq platform. The small RNA libraries were prepared with an Illumina TruSeq Small RNA sample preparation kit according to the manufacturer's

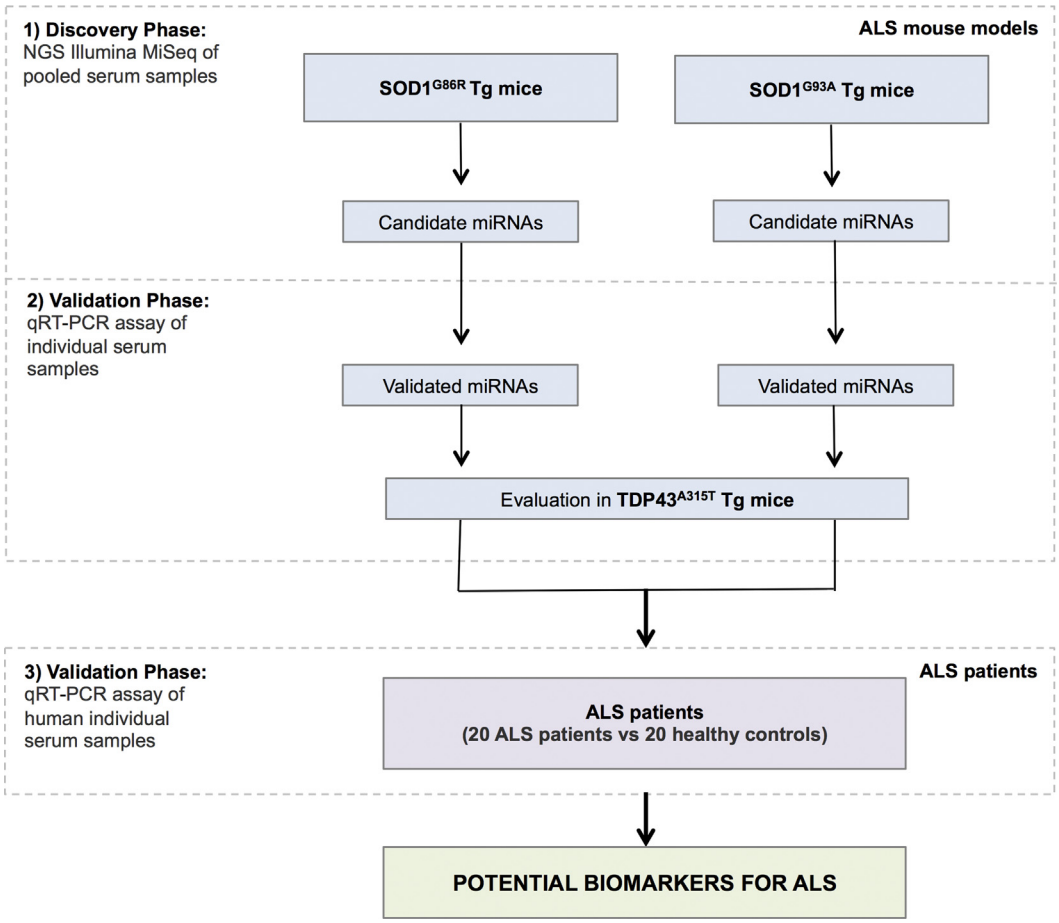

Fig. 1. Work flow of the experimental design. To identify novel miRNAs that are altered in ALS, we first performed NGS of different pools of serum samples derived from 2 SOD1 transgenic mouse models during late presymptomatic (P90) and a symptomatic disease stage and their respective littermate controls. Serum samples from SOD1^{G86R} were pooled (n = 5 animals per pool; C57JL/6 background) and from SOD1^{G93A} (n = 5 animals per pool; B6SJL mixed background) transgenic mouse and nontransgenic littermate control animals (n = 5 animals per pool). Candidate miRNAs were validated by qRT-PCR of individual animals (n = 5 per group) followed by the analysis of TDP-43 mutant transgenic mice. Then, the selected miRNAs were further measured in serum samples from sALS patients. Abbreviations: ALS, amyotrophic lateral sclerosis; miRNA, microRNA; NGS, next-generation sequencing.

protocol. Briefly, starting from 6 ng of total RNA from each sample (pooled serum samples), 3′ and 5′ adapters were sequentially ligated to each end of the RNA molecules (miRNAs and others small RNAs), followed by a reverse transcription reaction to generate single-stranded cDNA. The cDNA was then polymerase chain reaction (PCR) amplified by 15 cycles with 2 primers annealing to the ends of the adapters. The PCR product was selected by size using gel purification and validated using a DNA 1000 chip on an Agilent Technologies 2100 Bioanalyzer. The cDNA libraries were pooled at equal concentrations and sequenced on an Illumina MiSeq sequencer for 36 cycles of single-end sequencing.

2.6. Bioinformatics analysis of sequencing data

Sequencing reads were trimmed removing the 3′ adapter (TGGAATTCTCGGGTGCC AAGG) using Cutadapt v1.9 (Marcel, 2011). All reads shorter than 18 nucleotides (after adapter cleaning) were removed and high-quality (HQ) reads were selected using the NGS QC Toolkit v2.3.3 (Patel and Jain, 2012). Reads were considered as HQ reads, if 90% of the read had a quality Phred score of more than 30 on average. The adapter-cleaned HQ reads were mapped against the mouse genome sequence (UCSC assembly version mm10) using Bowtie (Langmead, 2010). In this step, the unique mapping filter (option -m 1) was used and to guarantee the best alignment for each read, the Bowtie options, “best” and “strata,” were applied. The miRNAs were annotated using the genomic coordinates overlapping of each aligned read against the miRNA coordinates retrieved from the miRBase v21 database (Kozomara and Griffiths-Jones, 2014). Furthermore, to annotate a higher number of sncRNAs, the coordinates for sncRNAs from NONCODE v4 (Xie et al., 2014) and fRNAdb (Kin et al., 2007) databases were also used. Considering only the reads that could be unequivocally identified as miRNAs, hierarchical clustering was performed using mean-normalized read counts transformed to logarithmic scale and then visualized using the R package gplots (R package version 2.16). To select differentially expressed miRNAs, read counts were normalized by dividing each read count by the total number of unique mapping reads in each condition. The fold change (FC) was manually calculated dividing the normalized expression values of the transgenic mouse by the normalized expression values of the Non-Tg mouse (e.g., SOD1^{G86R}/Non-Tg) for the late presymptomatic and symptomatic stages. We regarded an FC of more than 2 fold as biologically meaningful; however, a *p*-value could not be estimated due to pooling of the serum samples. Thus, we set the FC threshold at 2.0 and selected a group of those miRNAs that we found as differentially expressed in each stage for further validation by qRT-PCR in mice and humans. Furthermore, given that our main goal is to assess the usefulness of a translational approach based on ALS transgenic mouse models, we performed an evolutionary conservation analysis between the sequences of the deregulated miRNAs

found in the NGS study using mouse models and the presence of these candidates in the human genome. This information was used to select the deregulated miRNAs for validation as possible biomarkers in serum from ALS patients. Briefly, we performed a conservational analysis by mapping deregulated murine miRNAs against the human genome sequence (UCSC assembly version hg19) and by genomic coordinates overlapping with the Transmap EST data set (Rhead et al., 2010) allowing us to do synteny-filtered pairwise genome alignments between human and mouse sequences.

2.7. Circulating miRNA detection by quantitative RT-PCR

The TaqMan MicroRNA Reverse Transcription Kit and TaqMan MicroRNA assays (both from Applied Biosystems, Foster City, CA) were used for qRT-PCR of circulating miRNAs (Chen et al., 2005). Briefly, 3 μL of total RNA was reverse transcribed into cDNA. Given the low levels of total RNA detected in human samples, we used a cDNA preamplification TaqMan kit before the PCR amplification (Le Carré et al., 2014). RT-PCR reactions for each miRNA (20 μL reaction volume) were performed in triplicate, and each 20-μL reaction mixture included 0.16 μL of the RT product. Reactions were performed using an Applied Biosystems StepOnePlus Real-Time PCR system in 96-well plates at 95 °C for 10 minutes, followed by 50 cycles of 95 °C for 15 seconds, and 60 °C for 1 minute. miRNA levels were normalized to those of the spiked in cel-miR-39, that served as an internal control. Measurements were normalized using the formula $2 - \Delta Ct$, where $\Delta Ct = Ct(\text{miRNA test}) - Ct(\text{cel-miR-39})$. For calculating relative expression levels, the $\Delta\Delta Ct$ method was used. All used primers were obtained from Life Technologies Company.

2.8. Prediction and enrichment analysis of the target genes of miRNAs

We used the Ingenuity Pathway Analysis (IPA) software (Ingenuity Systems, Redwood City, CA, USA) to identify putative miRNA target genes and explore downstream biological pathways. Only circulating miRNAs that were found to be differentially expressed ($p < 0.05$) in the serum of ALS patients compared to healthy controls (hsa-miR-142-3p and hsa-miR-1249-3p) were included in this analysis. Specifically, we used the miRNA Target Filter tool, which links predicted and experimentally validated mRNA targets to each miRNA from the databases or softwares TarBase, miRecords, and TargetScan. Possible target genes of the hsa-miR-142-3p, which were found to be associated to ALS, were used to build an interaction network of miRNA and its target genes. The identified target genes were used to recognize those genes that were overrepresented (enriched) in certain canonical pathways using IPA core analysis. The association between the predicted mRNAs and the IPA canonical pathway was determined using 2 parameters: (1) *p*-value calculated using Fischer's exact test defining the probability that the association between the predicted mRNAs and the canonical pathway is due by chance and (2) a ratio of the number of predicted mRNAs that map to the pathway divided by the total number of genes that map to the canonical pathway.

2.9. Statistical analyses

The data distribution was assessed using Shapiro-Wilk test. For the comparison of categorical variables between ALS patients and healthy controls (such as sex and cardiovascular risk factors), the analysis was performed using Fisher's exact test. For comparison of continuous variables, specifically miRNA expression levels, between ALS transgenic and Non-Tg mice or ALS patients and healthy controls, we used unpaired Student's *t*-test. The comparison of miRNAs expression levels between early presymptomatic, late presymptomatic, and symptomatic stages was performed using analysis of variance with Bonferroni post hoc analysis. Correlation analysis between miRNA expression levels and clinical and biochemical parameters from ALS patients was performed using Pearson correlation coefficient. Receiver operating characteristic (ROC) curves and the area under the curve (AUC) were calculated to assess the ability of each miRNA to differentiate between ALS patients and healthy controls. To explore the diagnostic accuracy of the combination of multiple serum miRNAs (hsa-miR-142-3p plus hsa-miR-1249-3p), a combined ROC curve was performed by multiple logistic regression analysis. An AUC of 0.5 indicates classifications assigned by chance. Differences were considered statistically significant at a value of $p < 0.05$. All statistical analyses were performed using programs GraphPad 5.0 (GraphPad Software Inc., CA, USA) and Stata 12.0 (College Station, TX. StataCorp LP).

3. Results

3.1. Genome-wide expression profiling using NGS of miRNAs in serum from 2 SOD1 transgenic mouse models

Based on the heterogeneity of previously identified miRNAs in ALS models and patients, we developed a strategy to uncover common miRNAs that are altered in 2 transgenic mouse models independently of the specific genetic mutation studied and the genetic background. This screening was followed by validation in a different ALS mouse model in addition to blood samples derived from sALS patients (see work flow of the study in Fig. 1). To this end, we analyzed the global expression profile of circulating miRNAs in the serum from 2 SOD1 transgenic mouse models using NGS of sncRNAs isolated from pooled serum samples at 2 different disease stages, late presymptomatic (n = 5 animals) and symptomatic (n = 5 animals). During the discovery phase, pooling strategy was used to assess global serum miRNA profiles rather than having specific data for single mouse. We studied 2 independent ALS mouse models with different genetic backgrounds corresponding to $SOD1^{G86R}$ (mouse gene corresponding to G85R human mutation) and $SOD1^{G93A}$ (transgenic mice that overexpress the human transgene), and their respective Non-Tg littermate control animals (n = 5 animals). All symptomatic animals showed significant weight loss and clinical signs of lower motor neuron dysfunction (Fig. 2A and B) as previously described (Matus et al., 2013; Wegorzewska et al., 2009). A total of 48,220,190 reads were generated from 8 cDNA libraries using a MiSeq sequencer (Illumina). The number of reads per samples ranged from 5,250,124 to 7,116,783 (Supplementary Table S1). After selecting HQ reads, sequences were mapped to the reference genome allowing us to align 3.0% of the reads on average (minimum 2.0% and maximum 5.7%). For most of our samples, the length distribution of the unique mapped reads was as expected for miRNA studies, with a peak at 22 nt, corresponding to the expected miRNA size (Bellingham et al., 2012; Shao et al., 2010) (Fig. 2C and D). The number of mature miRNAs per sample ranged from 321 to 454. In addition, we identified other classes of sncRNAs, including piwiRNAs and snoRNAs (Fig. 2E and F). Interestingly, we found some sncRNAs sharing multiple RNA class annotation, which could be explained by bifunctional RNAs (Ender et al., 2008), differences in the database annotations (Jalali et al., 2016), and sncRNAs transcribed from opposite strands (Jacquier, 2009). Moreover, 77% of all the mapped sncRNAs were not recognized as a specific subclass of sncRNAs, which probably represent other less characterized sncRNA classes such as tRNAs, siRNAs, and YRNAs, among others (Dhahbi et al., 2013; Lee et al., 2009). Specifically, recent reports showed that tRNA-derived fragments called 5′ tRNA halves are abundantly

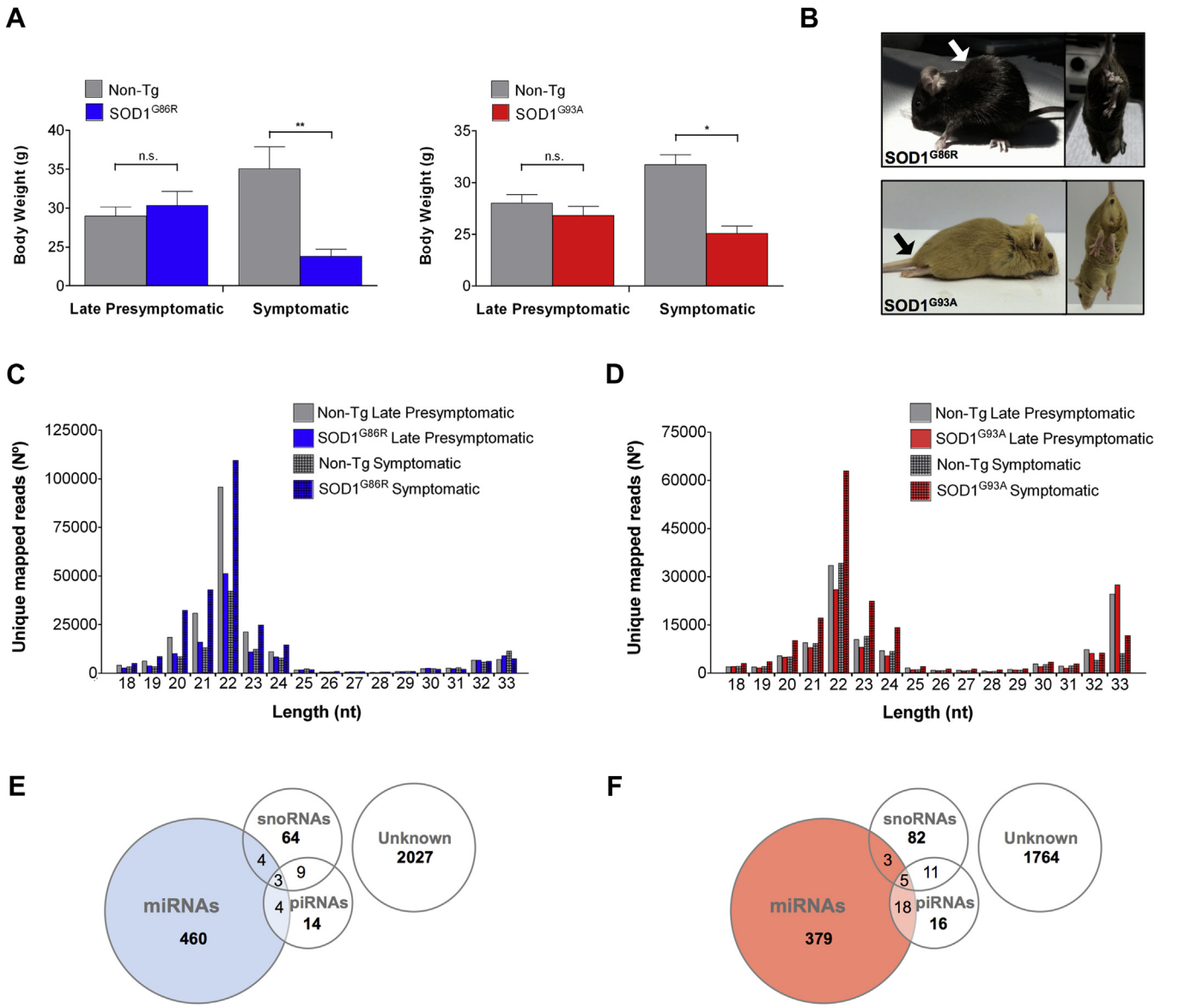

Fig. 2. Global analysis of circulating miRNAs in mutant SOD1 transgenic mice using NGS. (A) Body weight changes in SOD1^{G86R} and SOD1^{G93A} transgenic mice at late presymptomatic and symptomatic stages are shown compared to non-transgenic littermate control animals. Data are represented as mean and standard error. (B) ALS features in symptomatic SOD1^{G86R} and SOD1^{G93A} transgenic mice, specifically backbone arching and leg paresis (arrows). (C and D) Length distribution of uniquely mapped reads from NGS data obtained from SOD1^{G86R} and SOD1^{G93A} transgenic mice. (E and F) Total number of identified sncRNAs in SOD1^{G86R} (E) and SOD1^{G93A} (F) transgenic mice, including late presymptomatic and symptomatic stages. Subgroups of the sncRNAs, namely miRNAs, snoRNAs, piRNAs, and an unclassified subgroup (= unknown) are presented. Statistical analyses were performed using Student's t test. *p*-values: n.s., nonsignificant; * $p \leq 0.05$; ** $p \leq 0.01$. Abbreviations: ALS, amyotrophic lateral sclerosis; miRNA, microRNA; NGS, next-generation sequencing; Non-Tg, non-transgenic; sncRNAs, small noncoding RNAs.

expressed in the mouse serum, consuming most of the sequencing reads (Van Goethem et al., 2016; Victoria et al., 2015). Finally, independently of the SOD1 mutation, disease stage or genetic background, mmu-miR-22-3p and mmu-miR-10-5p were the most abundant miRNAs detected in serum samples, with the number of unique mapped reads ranging from 8318 to 32,905 across all samples for mmu-miR-22-3p and 5076 to 16,917 across all samples for mmu-miR-10-5p (Supplementary Fig. S1).

3.2. Identification of differentially expressed miRNAs in serum from SOD1 transgenic mice

To determine differentially expressed miRNAs in experimental ALS, we compared the global profiles of circulating miRNAs in the serum of mutant SOD1 transgenic mice and Non-Tg controls derived from late presymptomatic and symptomatic stages. The overall levels of circulating miRNAs considerably differed between mutant SOD1 and Non-Tg mice (Fig. 3A and B). Interestingly, the 2 mutant SOD1 transgenic mouse models analyzed here presented lower levels of circulating miRNAs at the late presymptomatic stage than Non-Tg mice, whereas an opposite distribution was observed in the symptomatic stage.

From the 471 miRNAs detected in the NGS analysis in the SOD1^{G86R} transgenic mouse model, only 4 miRNAs were found to be differentially expressed at late presymptomatic stages, 2 of which were upregulated and 2 were downregulated in the serum from ALS mice compared to Non-Tg mice. In sharp contrast, 60 miRNAs were altered in the serum at the symptomatic stage, comprising 46 upregulated and 14 downregulated miRNAs from mutant SOD1 mice compared with Non-Tg animals. In the case of SOD1^{G93A}

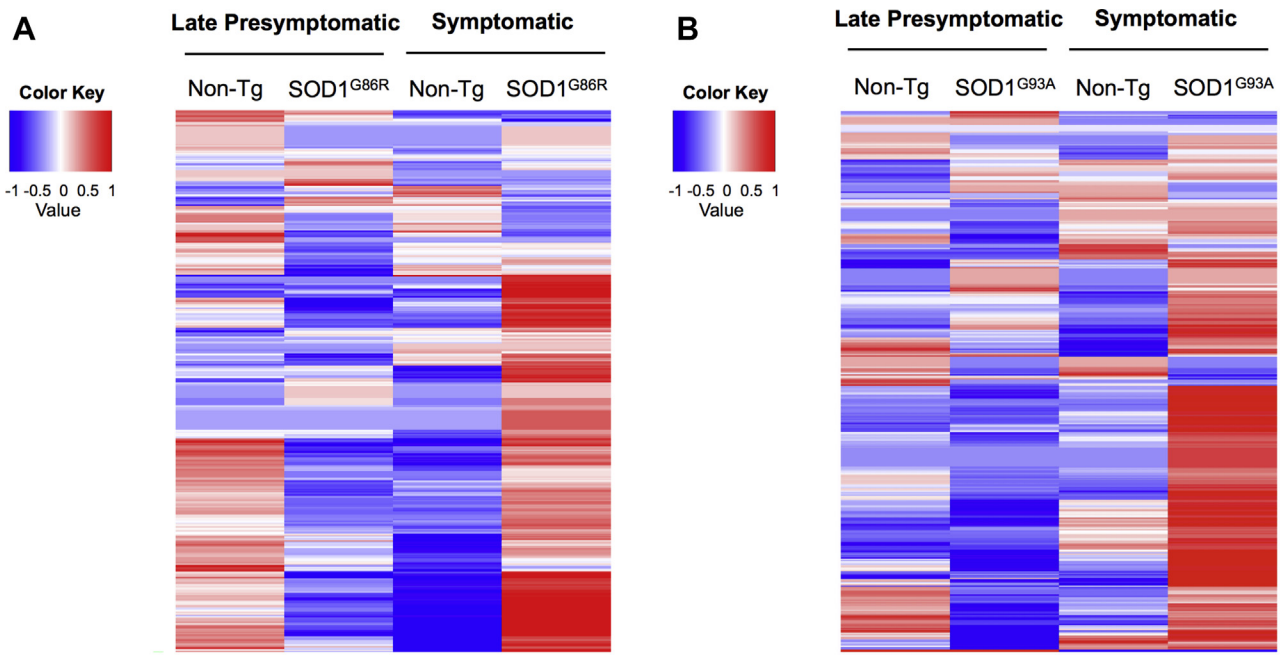

Fig. 3. Expression profile of circulating miRNAs in mutant SOD1 transgenic mice. (A and B) miRNAs were clustered using the means of normalized read counts for $SOD1^{G86R}$, $SOD1^{G93R}$ transgenic and Non-Tg mice. Heat maps are presented in logarithmic scale (log_2 fold change). The rows of the heat map represent miRNAs, while the columns represent $SOD1^{G86R}$, $SOD1^{G93R}$ transgenic and Non-Tg littermate controls. Heat maps were created using Heatmap.2 function from ggplot R package. Abbreviations: miRNA, microRNA; Non-Tg, non-transgenic.

transgenic mice, 405 miRNAs were detected in the NGS analysis, of which 26 miRNAs were affected in late presymptomatic $SOD1^{G93A}$ animals (22 upregulated and 4 downregulated in $SOD1^{G93A}$ mice), and 18 miRNAs were deregulated at the symptomatic stage (14 upregulated and 4 downregulated). Regarding the conservation analysis performed to all deregulated miRNAs (108 miRNAs), 89.8% of the mouse miRNAs presented conservation in humans (Supplementary Table S2).

Then, we determined the overlap between differentially expressed miRNAs in $SOD1^{G86R}$ and $SOD1^{G93A}$ models to identify miRNAs that are altered independently of the specific SOD1 mutation expressed. Surprisingly, only 2 miRNAs (mmu-miR-582-3p and mmu-miR-204-5p) were shared between our 2 experimental models of ALS in the late presymptomatic stage. Both miRNAs were upregulated in $SOD1^{G86R}$ animals and downregulated in the $SOD1^{G93A}$ model, respectively. At the symptomatic stage 2, miRNAs (mmu-miR-205-5p and mmu-miR-144-3p) were also shared between the 2 SOD1 mouse models analyzed, where mmu-miR-205-5p was downregulated in $SOD1^{G86R}$ mice and upregulated in $SOD1^{G93A}$ animals, while mmu-miR-144-3p was upregulated in both models. These findings suggest substantial global differences in the expression profiles of circulating miRNAs between $SOD1^{G86R}$ and $SOD1^{G93A}$ transgenic mouse models.

In summary, these results indicate a peripheral deregulation of circulating miRNAs in 2 ALS transgenic mouse models during late presymptomatic and symptomatic stages, with minimal overlap between $SOD1^{G86R}$ and $SOD1^{G93A}$ transgenic animals.

3.3. miRNAs in serum derived from mutant SOD1 mice

To select circulating miRNAs for further validation as ALS biomarkers, our validation strategy involved the quantification of relative miRNA levels of selected candidates by qRT-PCR of individual animals, monitoring an additional time point, and the further analysis of a different ALS model based on mutant TDP-43 overexpression. From the 108 differentially expressed miRNAs in the NGS analysis (Supplementary Table S2), we selected candidates according the following criteria: (1) high read counts, (2) high FC, and (3) conservation in humans. Applying these criteria, 7 miRNAs selected from $SOD1^{G86R}$ transgenic mice and 6 miRNAs selected from $SOD1^{G93A}$ transgenic mice were considered as candidate miRNA biomarkers and were further validated by qRT-PCR (Table 1). With this objective, we quantified the selected miRNAs in individual serum samples from 5 animals per group derived from $SOD1^{G86R}$ and $SOD1^{G93A}$ transgenic animals. The miRNAs selected were only validated in the mouse model where they were described; no cross-validation between SOD1 models was performed. Only 1 of the 13 selected miRNA candidates (mmu-miR-144-3p) did not amplify by qRT-PCR.

Table 1
Selected circulating miRNAs from next-generation sequencing study

MicroRNAs	Fold change
$SOD1^{G86R}$ Tg model	
Late presymptomatic stage	
mmu-miR-215-5p	−2.3
mmu-miR-375-3p	−2.3[a]
Symptomatic stage	
mmu-miR-142-3p	8.7[a]
mmu-let-7i-5p	4.2
mmu-miR-301a-3p	3.9
mmu-let-7f-5p	3.5
mmu-miR-205-5p	−4.7[a]
$SOD1^{G93A}$ Tg model	
Late presymptomatic stage	
mmu-miR-204-5p	−2.1[a]
mmu-miR-205-5p	−2.2
Symptomatic stage	
mmu-miR-144-3p	3.3
mmu-miR-183-5p	3.0[a]
mmu-miR-205-5p	3.0
mmu-miR-1249-3p	2.1[a]

[a] These circulating miRNAs were validated by qRT-PCR.

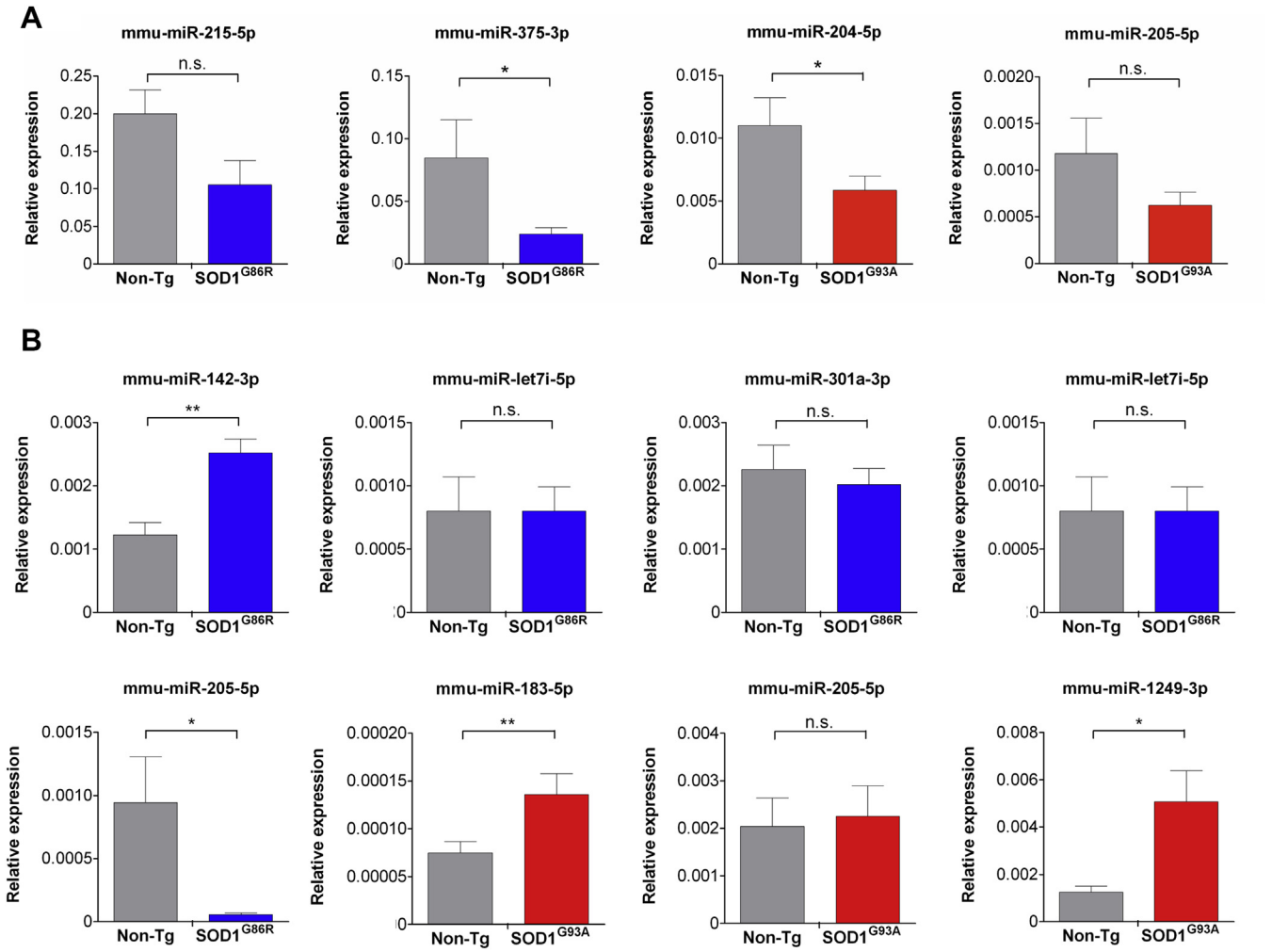

Fig. 4. Validation of selected circulating miRNAs in individual mutant SOD1 mice. Expression levels of selected circulating miRNAs in serum derived from $SOD1^{G86R}$ (blue bars) or $SOD1^{G93A}$ (red bars) mice; late presymptomatic stage (A) and symptomatic stage (B) were analyzed by real-time PCR and normalized to cel-miR-39 (n = 5 per group). Statistical analyses were performed using Student's t test. Mean and standard error is presented. *p* values: n.s., nonsignificant; * $p \leq 0.05$; ** $p \leq 0.01$. Abbreviations: miRNA, microRNA; PCR, polymerase chain reaction. (For interpretation of the references to color in this figure legend, the reader is referred to the Web version of this article.)

According to our validation, 3 of 7 miRNAs were confirmed to be significantly altered in $SOD1^{G86R}$ transgenic mice (Fig. 4). Specifically, mmu-miR-142-3p was upregulated and mmu-miR-205-5p was downregulated at the symptomatic stage in transgenic mice compared to controls, whereas mmu-miR-375-3p was downregulated during the late presymptomatic stage in transgenic mice. In the case of the $SOD1^{G93A}$ model, our validation experiments indicated that 3 of 6 miRNAs were altered (Fig. 4), showing upregulation of mmu-miR-183-5p and mmu-miR-1249-3p in symptomatic animals, whereas mmu-miR-204-5p was downregulated at the late presymptomatic stage. Importantly, we found a significant positive correlation ($r = 0.701$; $p = 0.01$) between the expression values (FC) of the measured candidate miRNAs using NGS and the relative expression levels quantified using qRT-PCR (Supplementary Fig. S2).

To further determine the changes across the progression of the diseases in these 2 experimental models of ALS, we then measured the levels of the 6 validated miRNAs at an additional time point that was considered as an early presymptomatic stage and during late presymptomatic and symptomatic stages for those miRNAs not validated during the other stages (Fig. 5). From the 3 miRNAs validated in the $SOD1^{G86R}$ model, the comparison between time points showed that mmu-miR-142-3p was specifically upregulated in the symptomatic stage, in contrast to mmu-miR-205-5p, which was downregulated in the same stage. For mmu-miR-375-3p, although the differential expression was not statistically significant between stages, its expression level was lower at late presymptomatic stages. From the 3 miRNAs validated in the $SOD1^{G93A}$ model, mmu-miR-183-5p and mmu-miR-1249-3p showed significant upregulation particularly in the symptomatic stage compared with early and late presymptomatic animals. mmu-miR-204-5p did not reach significant differences between the time points analyzed.

Finally, to increase the translational potential of our findings, we analyzed a different ALS transgenic model based on the expression of mutant $TDP43^{A315T}$ that is predicted to trigger neurodegeneration through an alternative molecular mechanism compared with mutant SOD1 mice (Wegorzewska et al., 2009). This mouse model develops progressive body weight loss, neuronal dysfunction, and motor problems accompanied by histological alteration in the frontal brain cortex; however, it does not develop evident paralysis (Wegorzewska et al., 2009). The analysis of the 6 validated miRNAs in SOD1 models using serum samples from symptomatic $TDP43^{A315T}$ animals indicated that only mmu-miR-204-5p was significantly differentially expressed, showing downregulation in $TDP43^{A315T}$ transgenic animals (Fig. 6). Overall, these

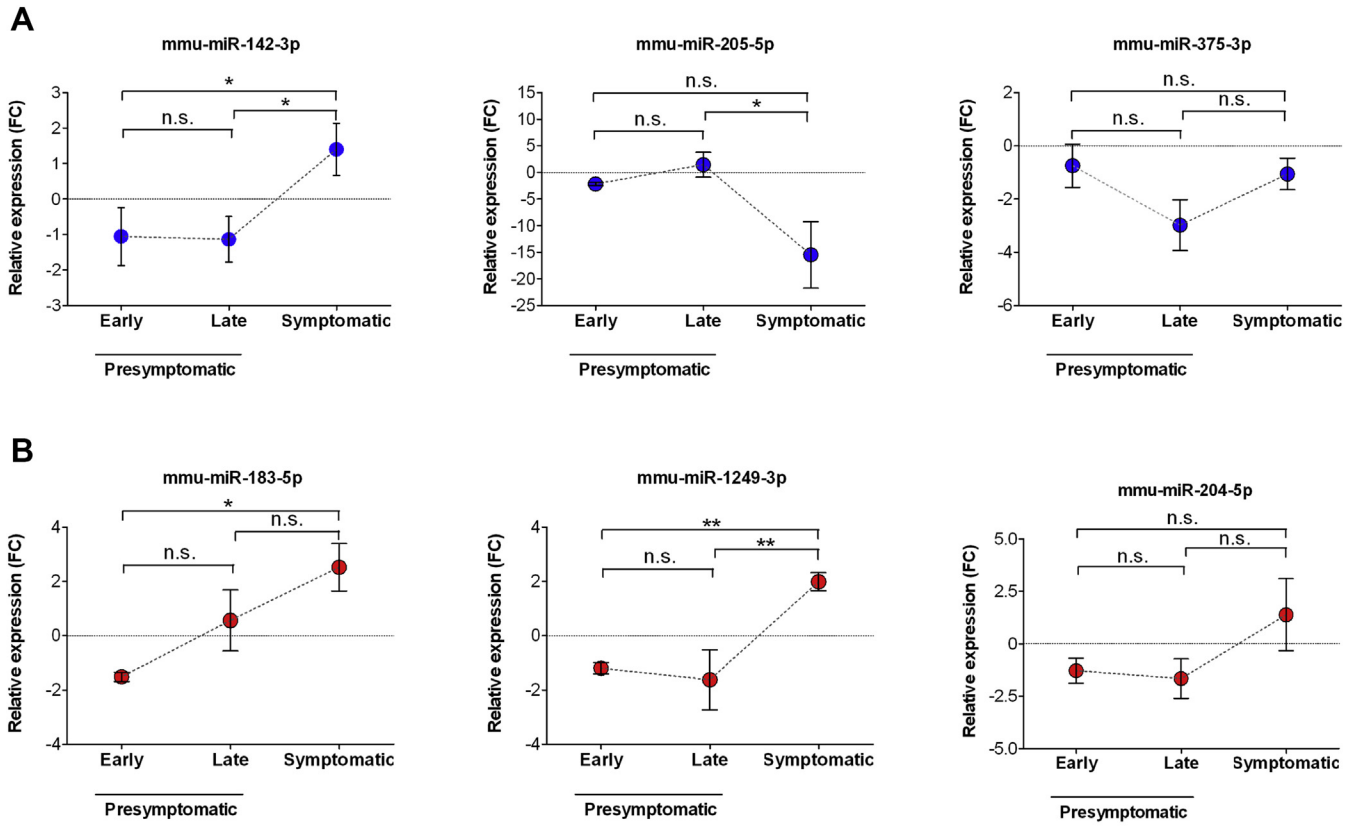

Fig. 5. Expression changes of validated circulating miRNAs during disease progression. Expression levels of validated circulating miRNAs in the serum of (A) $SOD1^{G86R}$ or (B) $SOD1^{G93A}$ mice during disease progression (early presymptomatic, late presymptomatic, and symptomatic stages) (n = 5 per group). Statistical analysis was performed using one-way ANOVA and Bonferroni correction for multiple testing. Data are presented as mean values and standard errors. *p*-values: n.s., nonsignificant; * $p \leq 0.05$; ** $p \leq 0.01$. Abbreviations: ANOVA, analysis of variance; FC, fold change of expression; miRNA, microRNA.

results suggest that individual miRNAs are significantly altered in various models of ALS, showing distinct expression patterns during the evolution of the disease.

3.4. Analysis of selected miRNAs in serum derived from sporadic ALS patients

After performing a comparative analysis of miRNA expression in 3 different ALS mouse models, we moved forward into evaluating possible changes in the 6 validated mouse miRNAs on serum samples derived from sALS cases. We enrolled 20 sALS patients and 20 healthy control subjects. The average age of sALS patients included in our study was 55 ± 10.6 years (range: 38–78 years), of which 9 were males and 11 females (Table 2). All patients were diagnosed with sALS and none of them had history or clinical examination suggestive of frontotemporal dementia. None of the sALS cases were receiving riluzole at recruitment. At the time of assessment, the mean disease duration time from symptom onset was 28.2 ± 15.1 months (range: 8–67 months) (Table 2). Bulbar-onset disease was evident in 20% of patients, while limb-onset disease accounted for 80% of patients with ALS. The median ALSFRS-R score was 30 (interquartile range: 16; range: 15–43) and the median Medical Research Council scale for testing muscle strength score was 44 (interquartile range: 18; range: 16–60). The clinical and hematological/biochemical test of ALS patients and control subjects are summarized in Supplementary Table S3.

We analyzed 6 miRNAs previously selected from our studies in ALS mouse models using qRT-PCR. Remarkably, altered levels of hsa-miR-142-3p and hsa-miR-1249-3p were observed in the serum from ALS patients compared to control subjects. Specifically, we found an upregulation of miR-142-3p and the downregulation of hsa-miR-1249-3p in patients with ALS compared to controls (Fig. 7A). Interestingly, miR-142-3p was also increased in $SOD1^{G86R}$ mice, which is in agreement with our findings in ALS patients. In contrast, although miR-1249-3p was also induced in the $SOD1^{G93A}$ transgenic mice, its levels were reduced in ALS patients. These results may suggest differences in the mechanisms involved in the circulating miRNA deregulation between mouse models and patients with ALS. Finally, no changes were observed in the expression levels of the other 4 miRNAs selected from mouse models when tested in ALS cases, including hsa-miR-204-5p, which was the only candidate altered in both $SOD1^{G93A}$ and $TDP43^{A315T}$ transgenic mice.

In summary, our findings support the identification of 2 new miRNAs that are deregulated in serum samples derived from mutant SOD1 mice and sALS patients.

3.5. Clinical correlations and ROC analysis for differentially expressed miRNAs in ALS patients

After validating the differential expression of miRNAs in human samples, we examined the correlation between the levels of the 2 identified miRNAs and clinical parameters. The expression levels of hsa-miR-142-3p, but not of hsa-miR-1249-3p, showed a significant negative correlation with ALSFRS-R ($r = -0.453$, $p = 0.041$) (Fig. 7B). Also, the expression levels of hsa-miR-142-3p and hsa-miR-1249-3p negatively correlate with serum CK levels, a peripheral blood marker of muscle damage (Supplementary Figs. S3 and S4). Other correlations tested using different disease parameters did not give positive outcomes (Supplementary Figs. S3 and S4). These results suggest

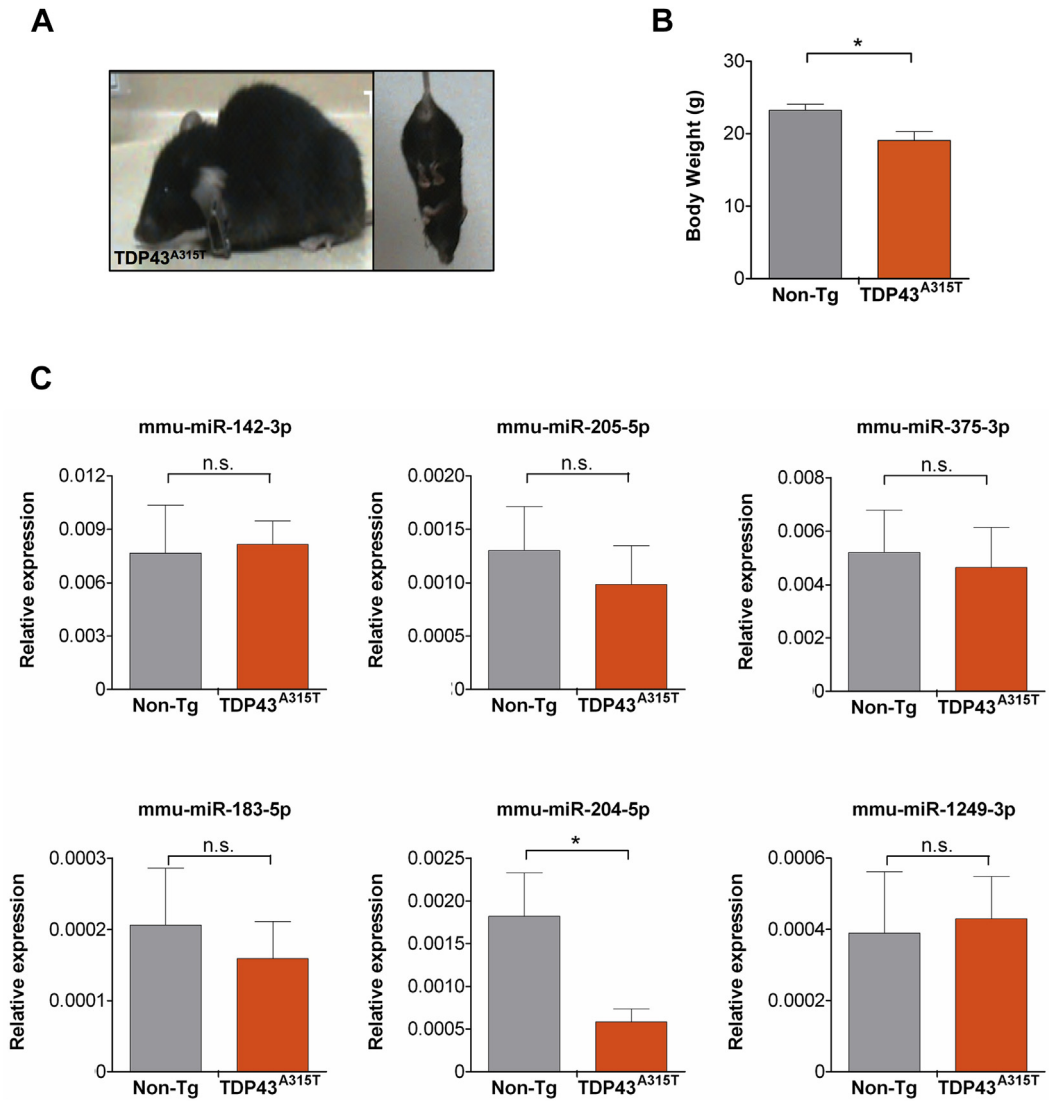

Fig. 6. Validation of circulating miRNAs in the serum of mutant TDP43 transgenic mice. (A) Disease features of symptomatic TDP43^{A315T} transgenic mice (backbone arching, muscle wasting, and paralysis). (B) Body weight changes in symptomatic TDP43^{A315T} transgenic mice. (C) Expression levels of indicated circulating miRNAs were quantified in serum samples obtained from symptomatic TDP43^{A315T} transgenic and non-transgenic littermate control animals (n = 6 per group) using real-time PCR. miRNA levels were normalized to cel-miR-39. Statistical analysis was performed using Student's t test. Mean and standard error is presented. *p*-values: n.s., nonsignificant; * $p \leq 0.05$. Abbreviations: miRNA, microRNA; PCR, polymerase chain reaction.

that hsa-miR-142-3p could be a possible biomarker of disease progression, which is unlikely to be released secondary to muscle destruction, given its negative correlation with CK levels.

In addition, ROC curves were separately obtained for each miRNA, and 1 ROC curve was established for the combination of the 2 validated miRNAs. The AUC for hsa-miR-142-3p was 0.713 (SE = 0.085) and for hsa-miR-1249-3p was 0.753 (SE = 0.083) (Fig. 7C). Furthermore, the AUC for the combination of the 2 miRNAs was 0.758, being similar to the AUC of each miRNA separately (Supplementary Fig. S5). Taken together, these results indicate that the identified miRNAs, alone or in combination, can discriminate between ALS patients and control subjects.

3.6. Target prediction of differentially expressed miRNAs and enrichment of canonical pathways in ALS patients

To predict possible target genes of hsa-miR-142-3p and hsa-miR-1249-3p, we took advantage of the miRNA Target Filter tool (IPA, Ingenuity). There were 554 possible target genes that are predicted to be regulated by hsa-miR-142-3p and 284 target genes predicted to be regulated by hsa-miR-1249-3p. Canonical pathway and functional network analysis of predicted targeted genes by hsa-miR-142-3p and hsa-miR-1249-3p were analyzed with IPA (Supplementary Table S4). From the 10 most significantly affected canonical pathways, we highlight the ones that may be directly involved in ALS pathogenesis: B cell receptor signaling, axonal guidance pathways, ephrin B signaling, and control of actin cytoskeleton (Table 3).

From the total target genes predicted to be regulated by hsa-miR-142-3p, 10 genes are associated with ALS, generating a significant enrichment of the IPA "ALS signaling" canonical pathway among the top 30 hits (−log [*p*-value] = 2.33E00 and ratio = 7.48E−02). These hits include (1) genes associated to mitochondrial dysfunction, endoplasmic reticulum stress, and apoptosis (*BCL2*, *BCL2L1*, *PIK3CG*, *PIK3R6*, *XIAP*, and *CASP12*); (2) genes associated to glutamate excitotoxicity (*CACNA1D*); and (3) ALS genes associated

Table 2
Clinical features of 20 patients with ALS

Patient	Age (y)	Sex	Disease duration (mo)	Region of onset	MRC sum score	ALSFRS-R	Progression rate	Awaji criteria
1	53	Male	26	LL	50	42	0.2	Probable
2	55	Male	16	LL	34	19	1.8	Definite
3	48	Female	25	UL	44	37	0.4	Definite
4	51	Male	8	UL	41	18	3.8	Definite
5	45	Female	24	LL	44	24	1	Probable
6	63	Female	36	UL	33	22	0.7	Definite
7	38	Female	19	LL	34	25	1.2	Probable
8	64	Female	67	UL	17	19	0.4	Definite
9	50	Male	48	UL	33	22	0.5	Definite
10	73	Female	29	UL	24	20	0.9	Definite
11	55	Male	14	UL	60	43	0.3	Probable
12	52	Male	17	LL	46	41	0.4	Probable
13	56	Female	36	Bulbar	55	38	0.3	Probable
14	45	Male	24	UL	53	36	0.5	Definite
15	68	Male	24	Bulbar	52	37	0.4	Probable
16	64	Male	57	LL	23	30	0.3	Definite
17	78	Female	36	Bulbar	49	30	0.5	Probable
18	56	Female	15	Bulbar	54	32	1.1	Probable
19	42	Female	13	LL	44	33	1.2	Definite
20	44	Female	30	LL	16	15	1.1	Definite
Mean	55		28.2		44.3	29.2	0.9	
SD	10.6		15.1		13	8.9	0.8	

Disease duration refers to the period from symptom onset to the date of blood samples collection.
The site of disease onset was classified as either UL, LL, or bulbar.
Muscle strength was clinically assessed using the MRC sum score. The total MRC sum score ranges from 0 (total paralysis) to 60 (normal strength). The score is the sum of the MRC score of 6 muscles (deltoid, biceps, wrist extensor, iliopsoas, quadriceps femoris, and tibialis anterior) on both sides, each muscle graded from 0 to 5.
The patients were clinically graded using the ALSFRS-R, with a maximum score of 48 when there is no disability.
The disease progression rate was calculated for each patient (PR = [48 − current ALSFRS-R score]/disease duration in months at recruitment) (see Material and methods).
Key: ALS, amyotrophic lateral sclerosis; ALSFRS-R, revised ALS functional rating; LL, lower limb; MRC, Medical Research Council; PR, progression rate; UL, upper limb.

to RNA metabolism, specifically *TDP-43* and *C9orf72*, 2 of the most relevant genes in ALS (Fig. 8). Taken together, this theoretical bioinformatics analysis suggests that hsa-miR-142-3p and hsa-miR-1249-3p may regulate a specific set of genes associated to the pathophysiology of ALS.

4. Discussion

There is an urgent need for biomarkers to diagnose neurodegenerative diseases and monitor their progression (Turner et al., 2009). The discovery of reliable ALS biomarkers is a crucial step for improving the diagnosis, correcting the classification of clinical subtypes, and evaluating the efficacy of new disease-modifying treatments (Bowser et al., 2011). miRNAs have been suggested as potential biomarkers for ALS (Freischmidt et al., 2015). In our present study, we identified global changes in the expression profile of circulating miRNAs in the serum of 2 different mutant SOD1 transgenic mice at the late presymptomatic and symptomatic disease stages. Our screening strategy allowed us to validate the selective alteration of 2 of these miRNAs in the serum of sALS patients. Furthermore, we found a negative correlation between the expression level of hsa-miR-142-3p and ALSFRS-R, suggesting an association between its expression level and disease progression. The bioinformatics prediction of putative target genes suggested a possible regulation of TDP-43 and C9orf72, 2 of the most relevant ALS factors, in addition to other genes related to axonal growth and ephrin signaling pathways.

In addition to ALS, alteration in the expression pattern of miRNAs has been described in multiple human diseases (Nicolas and Lopez-Martinez, 2010). Importantly, these changes in miRNAs levels are not restricted to the CNS, observing alteration including in blood cells and serum (Freischmidt et al., 2015; Kumar et al., 2013). Here, we identified low expression levels of circulating miRNA in late presymptomatic stage in 2 mutant SOD1 models that were then increased in the symptomatic stage. Zhou et al. (Zhou et al., 2013) performed an expression analysis of miRNAs in the spinal cord of $SOD1^{G93A}$ mouse at different disease stages using microarrays. In agreement with our findings, the authors observed a higher number of downregulated miRNAs at presymptomatic stages, a phenomenon that was reversed at the symptomatic stage, showing more upregulated than downregulated miRNAs. These findings suggest similar global changes in miRNA expression profiles between the CNS and peripheral compartments, such as the serum, in ALS mouse models. On the other hand, different studies done in humans have reported low expression levels of miRNAs in the spinal cord of ALS patients compared to control subjects (Campos-Melo et al., 2013; Figueroa-Romero et al., 2015), suggesting differences between mouse models and the disease in humans. From a pathophysiological point of view, the experimental ablation of Dicer and, in consequence, decrease in miRNAs levels have been associated with motor neuron degeneration and the development of spinal muscular atrophy phenotype (Haramati et al., 2010). Moreover, functional studies in vitro revealed that TDP-43 and FUS depletion generates decreased levels of miRNAs (Kawahara and Mieda-Sato, 2012; Morlando et al., 2012). Thus, miRNAs may directly contribute to the physiology of motor neurons, and hence, their deregulation may result in neuronal dysfunction and neurodegeneration.

It is important to highlight that the alterations in the global expression profile of circulating miRNAs are an early event occurring from the presymptomatic stages. These findings are consistent with the morphological and molecular changes observed in presymptomatic animals (Hegedus et al., 2008; van Zundert et al., 2008). Recently, Freischmidt et al. studied the expression profiles of circulating miRNAs in serum samples of asymptomatic SOD1, FUS, and C9orf72 mutation carriers. This study indicated a highly homogenous alteration of the miRNA profile in patients with fALS that was largely independent from the underlying disease causative gene. In addition, they identified 24 downregulated miRNAs in presymptomatic ALS mutation carriers up to 2 decades or more

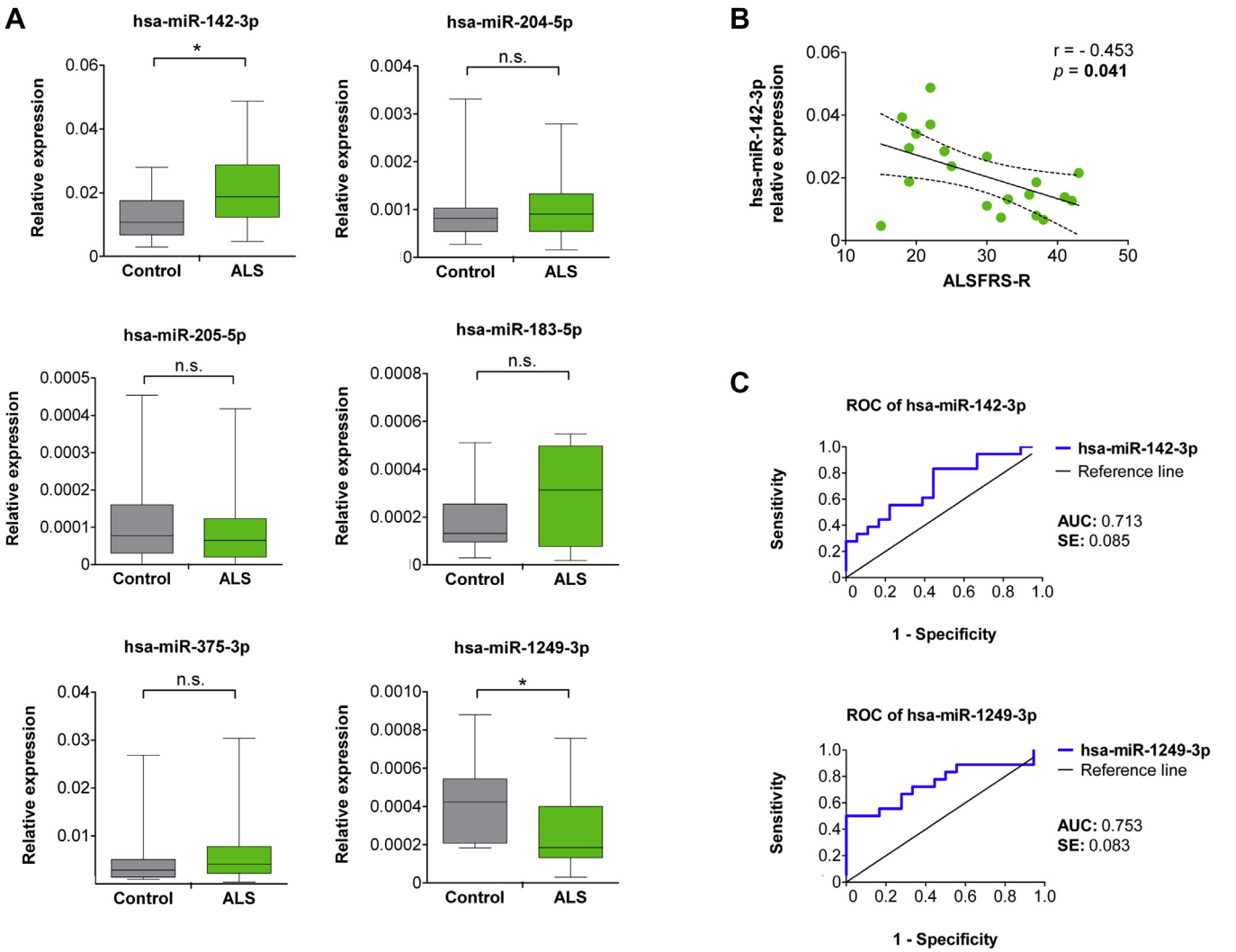

Fig. 7. Evaluation of validated miRNAs in serum samples of sporadic ALS patients. (A) Expression levels of validated circulating miRNAs in the serum of ALS patients (n = 20) and health control subjects (n = 20) using real-time PCR. miRNA levels were normalized to cel-miR-39. Statistical analysis was performed using Student's t test. The data were represented in a box plot, in which the box represents the interquartile range and arms the 5th and 95th percentile. (B) Correlation between hsa-miR-142-3p expression levels and ALSFRS-R (Pearson correlation coefficient). (C) ROC curve analysis using hsa-miR-142-3p and hsa-miR-1249-3p for discriminating ALS patients from healthy control subjects. *p* values: n.s., nonsignificant; * $p \leq 0.05$. Abbreviations: ALS, amyotrophic lateral sclerosis; ALSFRS-R, revised ALS functional rating; AUC, area under the ROC curve; miRNA, microRNA; PCR, polymerase chain reaction; ROC, receiver operating characteristic; SE, standard error.

before the estimated disease onset of which 91.7% miRNAs overlapped with the ones found in fALS patients (Freischmidt et al., 2014).

In our study, we found differences in the expression profiles of circulating miRNAs between mutant SOD1 mice. In addition, from the 6 circulating miRNAs validated in mice, only 2 of them (hsa-miR-142-3p and hsa-miR-1249-3p) reached statistical significance when they were evaluated in ALS patient samples. In addition, although hsa-miR-142-3p was upregulated in serum samples from $SOD1^{G86G}$ and ALS patients, analysis of hsa-miR-1249-3p indicated that it was induced in serum samples from $SOD1^{G93A}$ but was found downregulated in the serum of ALS patients, which may suggest temporal differences between the pathophysiological mechanisms involved in the circulating miRNA deregulation between mouse models and the disease in humans. This high variability between miRNAs identified in SOD1 mouse models and their validation in ALS patients verify the suggested partial ability to translate biological and therapeutic findings from transgenic mouse models to patients with ALS (Ittner et al., 2015). Despite the fact ALS mouse models reproduce most of the clinical and neuropathological findings of the disease, a recent study showed that mouse models rarely mimic the transcriptome of human neurodegenerative diseases (Burns et al., 2015). In addition, this report showed that mouse models frequently overexpressed genes associated with cellular stress that are actually consistently downregulated in patients with neurodegenerative diseases. All this evidence highlights the need of developing novel mouse models based not only on single mutations (such as SOD1 or TDP43 models) but also on new multifactorial damage models ("multiple hit" models). In the meantime, given the significant number of ALS mouse models available, further therapeutic and biomarker studies should include the combination of multiple animal models, with different genetic background before advancing into clinical studies in patients (Festing, 2010; Ittner et al., 2015).

We have found deregulation of hsa-miR-142-3p and hsa-miR-1249-3p in the serum of sALS patients. In agreement with our results, studies performed in the spinal cord of transgenic ALS mouse models and sALS and fALS patients also showed overexpression of miR-142-3p (Koval et al., 2013; Zhou et al., 2013), suggesting a strong association with ALS. Concerning other

Table 3
Top 10 canonical pathways of miR-142-3p and miR-1249-3p predicted target genes

Canonical pathways (IPA)	−log (*p*-value)	Ratio
miR-142-3p–predicted target genes		
Clathrin-mediated endocytosis signaling	7.43	1.06E−01
Molecular mechanisms of cancer	4.32	6.17E−02
Epithelial adherens junction signaling	3.56	8.11E−02
Protein kinase A signaling	3.48	5.53E−02
B cell receptor signaling	3.29	7.18E−02
CCR3 signaling in eosinophils	3.09	8.2E−02
Tight junction signaling	3.08	7.19E−02
Actin cytoskeleton signaling	2.96	6.33E−02
Breast cancer regulation by Stathmin1	2.95	6.6E−02
Dopamine-DARPP32 feedback in cAMP signaling	2.91	6.86E−02
miR-1249-3p–predicted target genes		
Axonal guidance signaling	2.52	2.96E−02
Ephrin B signaling	1.87	5.33E−02
Adipogenesis pathway	1.69	3.91E−02
Ephrin receptor signaling	1.66	3.39E−01
Glucose and glucose-1-phosphate degradation	1.61	1E−01
IL-22 signaling	1.47	8.33E−02
Role of JAK1, JAK2, and TYK2 in interferon signaling	1.47	8.33E−02
Oncostatin M signaling	1.19	5.88E−02
Role of JAK2 in hormone-like cytokine signaling	1.17	5.71E−02
Autophagy	1.07	5E−02

Key: cAMP, cyclic adenosine monophosphate; IPA, Ingenuity Pathway Analysis.

neurodegenerative diseases, 7 deregulated circulating miRNAs were reported to be altered in the plasma of patients with Alzheimer's disease, 1 of which was hsa-miR-142-3p (Kumar et al., 2013). In addition, different studies in multiple sclerosis patients have described augmented hsa-miR-142-3p levels in leukocytes and in CNS tissue (Junker et al., 2009; Keller et al., 2009). Besides its alteration in neurological diseases, circulating hsa-miR-142-3p is also modified in non-neurological diseases (Ellis et al., 2013; Makino et al., 2012; Ortega et al., 2014; Pivarcsi et al., 2013). Numerous studies have shown high expression of hsa-miR-142-3p in hematopoietic organs and cells (Chen et al., 2004; Gauwerky et al., 1989). Furthermore, ectopic expression of miR-142 has a profound effect on the differentiation of T lymphocytes (Wu et al., 2007). At the functional level, it was recently reported that miR-142 knock-out mice display multiple hematological alterations in both, the myeloid and lymphoid lineages (Shrestha et al., 2015). Differential expression of miR-142-3p has been associated with neuroinflammation and microglial activation (Chaudhuri et al., 2013; Naqvi et al., 2015), 2 relevant factors in ALS (Boillée et al., 2006; Zhao et al., 2010). Thus, it is possible that the upregulation of hsa-miR-142-3p in the serum of patients with sALS may be related in part with neuroinflammation. About hsa-miR-1249-3p, limited information is available regarding its potential role in human physiology and even less in neurological diseases. In summary, deregulation of hsa-miR-1249-3p has been described in cells and neoplastic tissue from small-cell carcinoma of the esophagus and hepatocellular carcinoma (Katayama et al., 2012; Okumura et al., 2015). Moreover, hsa-miR-1249-3p was recently reported to be differentially expressed in the plasma of patients with prediabetes and type 2 diabetes (Yan et al., 2016). However, until now, there was no previous association between hsa-miR-1249-3p and ALS.

Concerning the distribution and origin of circulating miRNAs in different body compartments, many hypotheses have been raised. A study that evaluated the expression levels of 10 TDP-43–associated miRNAs in ALS patients has found a poor correlation between serum and CSF miRNA expression levels (Freischmidt et al., 2013). The authors suggested the existence of independent regulatory mechanisms between the CSF and serum compartments. Moreover, Toivonen et al. have reported a significant overexpression of miR-206 in the serum of ALS patients (Toivonen et al., 2014). They described that miR-206 is preferably overexpressed in fast muscle fibers in SOD1^{G93A}. The authors suggest that a part of the deregulated pool of circulating miRNAs in ALS is released from muscle tissue. In contrast to the findings of Toivonen et al., we did not detect reads for miR-206 in our SOD1 mouse models, which might be explained by the different techniques and/or the different mouse genetic backgrounds used. Of further relevance, we found a negative correlation between the hsa-miR-142-3p expression levels and serum CK values, which argue against its possible release after muscle destruction.

Our bioinformatics analysis with IPA predicted that hsa-miR-142-3p may regulate TDP-43 and C9orf72 expressions. This is of special interest because both target genes play a pivotal role in ALS pathogenesis as well as the association between ALS and frontotemporal dementia (Ahmed et al., 2016). Target gene prediction for hsa-miR-1249-3p identified 2 overrepresented canonical pathways involved in axonal growth and ephrin B signaling pathways. According to the distal axonopathy hypothesis of ALS, alterations in the axonal growth may play a fundamental role in ALS as there is accumulating evidence suggesting that the earliest presymptomatic pathological changes occur distally in axons and at the neuromuscular junction (Moloney et al., 2014). Importantly, pharmacological and genetic inhibition of Epha4 signaling, a downstream component of ephrin-B3 (Himanen et al., 2004), rescues mutant SOD1-induced phenotypes in zebrafish and increases the survival rate in rat and mouse models of ALS (Paixão et al., 2013; Van Hoecke et al., 2012). This evidence supports the idea that miR-1249-3p may have relevant roles in ALS disease development, a hypothesis that remains to be tested.

Our findings suggest the existence of a systemic deregulation of miRNAs in the serum of mutant SOD1 mouse models and sALS patients. Growing evidence highlights the fact that ALS is a systemic disease, involving changes in metabolism, immune responses, and connective tissue (Dupuis et al., 2004; Hovden et al., 2013; Kolde et al., 1996). The systemic deregulation of miRNAs may also reflect the dysfunction of the peripheral nerve, neuromuscular junctions, and/or muscle alterations in ALS patients. Based on the high variability of hits identified in independent studies, it is predicted that a combination of various miRNAs, such as the ones identified here, together with additional molecules may be required to fingerprint ALS at the molecular level. Such a panel of miRNAs could serve as a signature reflecting disease progression and might help to distinguish ALS from ALS-mimicking diseases. Validation of our results in large patient cohorts (cross-sectional and longitudinal studies) including genetic and sporadic cases with different clinical phenotypes and disease stages may contribute to further increase the value of the miRNAs identified here as possible tools to diagnose ALS and monitor its progression.

Disclosure statement

The authors have no actual or potential conflicts of interest.

Acknowledgements

The authors thank Javiera Ponce for technical support as an animal care supervisor. The authors would also like to thank the clinicians who referred patients to be recruited in this study, including Dr Mario Campero (Clinica Las Condes and Hospital Clínico Universidad de Chile, Santiago, Chile), Dr Mario Rivera (Clinica Davila, Santiago, Chile), Dr Gabriel Cea (Hospital del Salvador, Universidad de Chile, Santiago, Chile), Dr Patricia Lillo (Hospital Barros Luco Trudeau, Universidad de Chile, Santiago, Chile), and Dr Daniel Valenzuela (Hospital Barros Luco Trudeau,

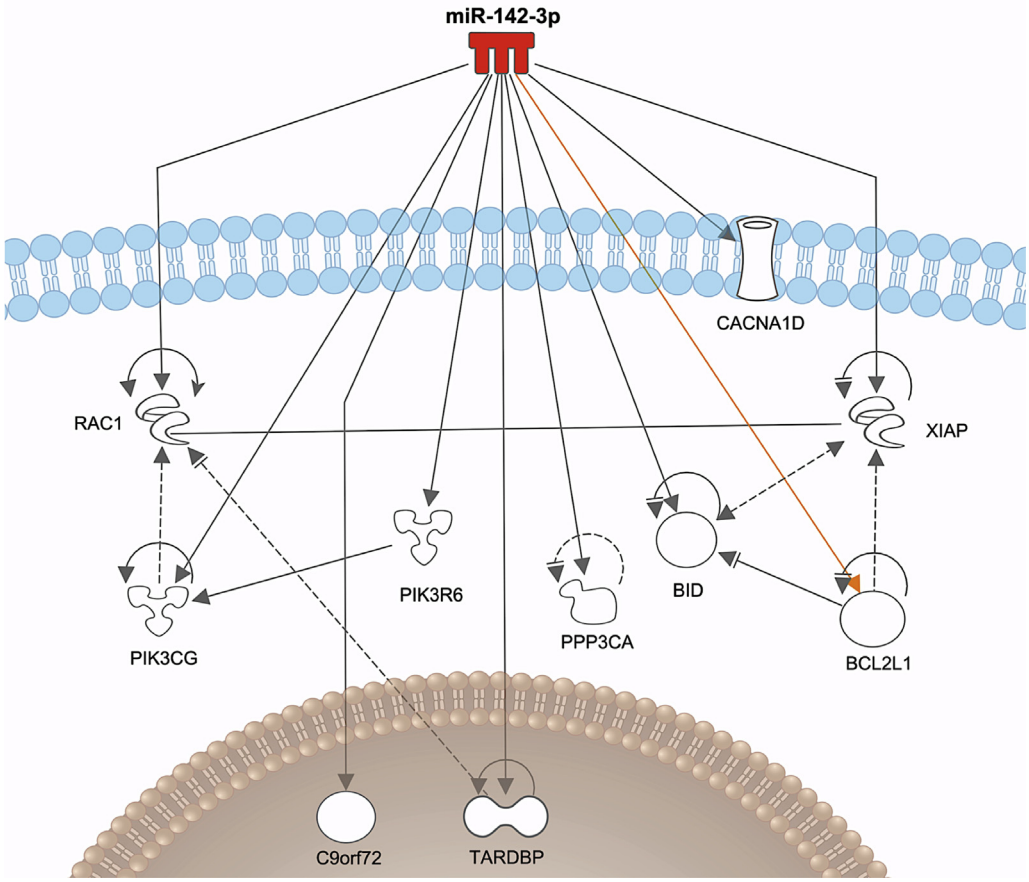

Fig. 8. Molecular gene networks of ALS-associated genes potentially modulated by miR-142-3p. Target genes potentially regulated by hsa-miR-142-3p were determined using the miRNA Target Filter tool of the software IPA. Ten genes associated with ALS are presented as a gene network. Red represents miRNA overexpression (here, overexpressed miR-142-3p). Black lines indicate miRNAs/mRNA interactions. Orange line represents regulation of a target gene, experimentally validated by other research groups. Gray lines (solid and dashed) represent structural or functional relationships between genes or their encoded proteins. Abbreviations: ALS, amyotrophic lateral sclerosis; IPA, Ingenuity Pathway Analysis; miRNA, microRNA. (For interpretation of the references to color in this figure legend, the reader is referred to the Web version of this article.)

Universidad de Chile, Santiago, Chile). This work was funded by Millennium Institute No. P09-015-F, FONDAP program 15150012, the Frick Foundation 20014-15, ALS Therapy Alliance 2014-F-059, Muscular Dystrophy Association 382453, CONICYT-USA 2013-0003, Michael J Fox Foundation for Parkinson's Research–Target Validation grant No 9277, COPEC-UC Foundation 2013.R.40, Ecos-Conicyt C13S02, FONDECYT No. 1140549, Office of Naval Research-Global (ONR-G) N62909-16-1-2003, and ALSRP Therapeutic Idea Award AL150111 (Claudio Hetz). FONDECYT No. 1161284 (Soledad Matus), CONICYT master fellowship No. 22130888 (Leslie Bargted). CONICYT Ring Initiative ACT1109 (Patricio Manque, Claudio Hetz, Soledad Matus). ALS Therapy Alliance-2014-F-034 and CONICYT DRI USA 2013-0030 (Brigitte van Zundert). Doctoral Fellowships from CONICYT 21151265 (Sebastian Abarzua).

Authors' contributions: JMM, PM, and CH planned the experiments, interpreted the data, and prepared the manuscript. JMM, CS, MU, LB, SM, and SA carried out the experiments. JMM, RA-C, and VM-C did the bioinformatics analysis. RV and BVZ supervised the project and gave conceptual input. All authors read and approved the final manuscript.

Appendix A. Supplementary data

Supplementary data associated with this article can be found, in the online version, at https://doi.org/10.1016/j.neurobiolaging.2017.12.020.

References

Abe, M., Bonini, N.M., 2013. MicroRNAs and neurodegeneration: role and impact. Trends Cell. Biol. 23, 30–36.
Ahmed, R.M., Irish, M., Piguet, O., Halliday, G.M., Ittner, L.M., Farooqi, S., Hodges, J.R., Kiernan, M.C., 2016. Amyotrophic lateral sclerosis and frontotemporal dementia: distinct and overlapping changes in eating behaviour and metabolism. Lancet Neurol. 15, 332–342.
Al-Chalabi, A., Hardiman, O., Kiernan, M.C., Chiò, A., Rix-Brooks, B., van den Berg, L.H., 2016. Amyotrophic lateral sclerosis: moving towards a new classification system. Lancet Neurol. 15, 1182–1194.
Arroyo, J.D., Chevillet, J.R., Kroh, E.M., Ruf, I.K., Pritchard, C.C., Gibson, D.F., Mitchell, P.S., Bennett, C.F., Pogosova-Agadjanyan, E.L., Stirewalt, D.L., Tait, J.F., Tewari, M., 2011. Argonaute2 complexes carry a population of circulating microRNAs independent of vesicles in human plasma. Proc. Natl. Acad. Sci. U. S. A. 108, 5003–5008.
Bartel, D.P., 2009. MicroRNAs: target recognition and regulatory functions. Cell 136, 215–233.
Bellingham, S.A., Coleman, B.M., Hill, A.F., 2012. Small RNA deep sequencing reveals a distinct miRNA signature released in exosomes from prion-infected neuronal cells. Nucleic Acids Res. 40, 10937–10949.
Benigni, M., Ricci, C., Jones, A.R., Giannini, F., Al-Chalabi, A., Battistini, S., 2016. Identification of miRNAs as potential biomarkers in cerebrospinal fluid from amyotrophic lateral sclerosis patients. Neuromolecular Med. 18, 551–560.
Boillée, S., Vande Velde, C., Cleveland, D.W., 2006. ALS: a disease of motor neurons and their nonneuronal neighbors. Neuron 52, 39–59.
Bowser, R., Turner, M.R., Shefner, J., 2011. Biomarkers in amyotrophic lateral sclerosis: opportunities and limitations. Nat. Rev. Neurol. 7, 631–638.
Buratti, E., De Conti, L., Stuani, C., Romano, M., Baralle, M., Baralle, F., 2010. Nuclear factor TDP-43 can affect selected microRNA levels. FEBS J. 277, 2268–2281.
Burns, T.C., Li, M.D., Mehta, S., Awad, A.J., Morgan, A.A., 2015. Mouse models rarely mimic the transcriptome of human neurodegenerative diseases: a systematic bioinformatics-based critique of preclinical models. Eur. J. Pharmacol. 759, 101–117.

Campos-Melo, D., Droppelmann, C.A., He, Z., Volkening, K., Strong, M.J., 2013. Altered microRNA expression profile in amyotrophic lateral sclerosis: a role in the regulation of NFL mRNA levels. Mol. Brain 6, 26.
Castillo, K., Nassif, M., Valenzuela, V., Rojas, F., Matus, S., Mercado, G., Court, F.A., van Zundert, B., Hetz, C., 2013. Trehalose delays the progression of amyotrophic lateral sclerosis by enhancing autophagy in motoneurons. Autophagy 9, 1308–1320.
Cedarbaum, J.M., Stambler, N., Malta, E., Fuller, C., Hilt, D., Thurmond, B., Nakanishi, A., 1999. The ALSFRS-R: a revised ALS functional rating scale that incorporates assessments of respiratory function. BDNF ALS Study Group (Phase III). J. Neurol. Sci. 169, 13–21.
Chaudhuri, A.D., Yelamanchili, S.V., Marcondes, M.C.G., Fox, H.S., 2013. Up-regulation of microRNA-142 in simian immunodeficiency virus encephalitis leads to repression of sirtuin1. FASEB J. 27, 3720–3729.
Chen, C.-Z., Li, L., Lodish, H.F., Bartel, D.P., 2004. MicroRNAs modulate hematopoietic lineage differentiation. Science 303, 83–86.
Chen, C., Ridzon, D.A., Broomer, A.J., Zhou, Z., Lee, D.H., Nguyen, J.T., Barbisin, M., Xu, N.L., Mahuvakar, V.R., Andersen, M.R., Lao, K.Q., Livak, K.J., Guegler, K.J., 2005. Real-time quantification of microRNAs by stem-loop RT-PCR. Nucleic Acids Res. 33, e179.
Chiò, A., 1999. ISIS Survey: an international study on the diagnostic process and its implications in amyotrophic lateral sclerosis. J. Neurol. (246 Suppl), III1–III5.
de Carvalho, M., Dengler, R., Eisen, A., England, J.D., Kaji, R., Kimura, J., Mills, K., Mitsumoto, H., Nodera, H., Shefner, J., Swash, M., 2008. Electrodiagnostic criteria for diagnosis of ALS. Clin. Neurophysiol. 119, 497–503.
De Felice, B., Guida, M., Guida, M., Coppola, C., De Mieri, G., Cotrufo, R., 2012. A miRNA signature in leukocytes from sporadic amyotrophic lateral sclerosis. Gene 508, 35–40.
De Felice, B., Annunziata, A., Fiorentino, G., Borra, M., Biffali, E., Coppola, C., Cotrufo, R., Brettschneider, J., Giordana, M.L., Dalmay, T., Wheeler, G., D'Alessandro, R., 2014. miR-338-3p is over-expressed in blood, CFS, serum and spinal cord from sporadic amyotrophic lateral sclerosis patients. Neurogenetics 15, 243–253.
Dhahbi, J.M., Spindler, S.R., Atamna, H., Boffelli, D., Mote, P., Martin, D.I.K., 2013. 5'-YRNA fragments derived by processing of transcripts from specific YRNA genes and pseudogenes are abundant in human serum and plasma. Physiol. Genomics 45, 990–998.
Dupuis, L., Oudart, H., René, F., Gonzalez de Aguilar, J.-L., Loeffler, J.-P., 2004. Evidence for defective energy homeostasis in amyotrophic lateral sclerosis: benefit of a high-energy diet in a transgenic mouse model. Proc. Natl. Acad. Sci. U. S. A. 101, 11159–11164.
Ellis, K.L., Cameron, V.A., Troughton, R.W., Frampton, C.M., Ellmers, L.J., Richards, A.M., 2013. Circulating microRNAs as candidate markers to distinguish heart failure in breathless patients. Eur. J. Heart Fail. 15, 1138–1147.
Emde, A., Eitan, C., Liou, L.-L., Libby, R.T., Rivkin, N., Magen, I., Reichenstein, I., Oppenheim, H., Eilam, R., Silvestroni, A., Alajajian, B., Ben-Dov, I.Z., Aebischer, J., Savidor, A., Levin, Y., Sons, R., Hammond, S.M., Ravits, J.M., Möller, T., Hornstein, E., 2015. Dysregulated miRNA biogenesis downstream of cellular stress and ALS-causing mutations: a new mechanism for ALS. EMBO J. 34, 2633–2651.
Ender, C., Krek, A., Friedländer, M.R., Beitzinger, M., Weinmann, L., Chen, W., Pfeffer, S., Rajewsky, N., Meister, G., 2008. A human snoRNA with MicroRNA-like functions. Mol. Cell. 32, 519–528.
Esmaeili, M.A., Panahi, M., Yadav, S., Hennings, L., Kiaei, M., 2013. Premature death of TDP-43 (A315T) transgenic mice due to gastrointestinal complications prior to development of full neurological symptoms of amyotrophic lateral sclerosis. Int. J. Exp. Pathol. 94, 56–64.
Festing, M.F.W., 2010. Improving toxicity screening and drug development by using genetically defined strains. Methods Mol. Biol. 602, 1–21.
Figueroa-Romero, C., Hur, J., Simon Lunn, J., Paez-Colasante, X., Bender, D.E., Yung, R., Sakowski, S.A., Feldman, E.L., 2015. Expression of microRNAs in human post-mortem amyotrophic lateral sclerosis spinal cords provides insight into disease mechanisms. Mol. Cell. Neurosci. 71, 34–45.
Freibaum, B.D., Lu, Y., Lopez-Gonzalez, R., Kim, N.C., Almeida, S., Lee, K.-H., Badders, N., Valentine, M., Miller, B.L., Wong, P.C., Petrucelli, L., Kim, H.J., Gao, F.-B., Taylor, J.P., 2015. GGGGCC repeat expansion in C9orf72 compromises nucleocytoplasmic transport. Nature 525, 129–133.
Freischmidt, A., Müller, K., Ludolph, A.C., Weishaupt, J.H., 2013. Systemic dysregulation of TDP-43 binding microRNAs in amyotrophic lateral sclerosis. Acta Neuropathol. Commun. 1, 42.
Freischmidt, A., Müller, K., Zondler, L., Weydt, P., Volk, A.E., Božič, A.L., Walter, M., Bonin, M., Mayer, B., von Arnim, C.A.F., Otto, M., Dieterich, C., Holzmann, K., Andersen, P.M., Ludolph, A.C., Danzer, K.M., Weishaupt, J.H., 2014. Serum microRNAs in patients with genetic amyotrophic lateral sclerosis and pre-manifest mutation carriers. Brain 137, 2938–2950.
Freischmidt, A., Müller, K., Zondler, L., Weydt, P., Mayer, B., von Arnim, C.A.F., Hübers, A., Dorst, J., Otto, M., Holzmann, K., Ludolph, A.C., Danzer, K.M., Weishaupt, J.H., 2015. Serum microRNAs in sporadic amyotrophic lateral sclerosis. Neurobiol. Aging 1–6.
Gal, J., Kuang, L., Barnett, K.R., Zhu, B.Z., Shissler, S.C., Korotkov, K.V., Hayward, L.J., Kasarskis, E.J., Zhu, H., 2016. ALS mutant SOD1 interacts with G3BP1 and affects stress granule dynamics. Acta Neuropathol. 132, 563–576.
Gauwerky, C.E., Huebner, K., Isobe, M., Nowell, P.C., Croce, C.M., 1989. Activation of MYC in a masked t(8;17) translocation results in an aggressive B-cell leukemia. Proc. Natl. Acad. Sci. U. S. A. 86, 8867–8871.
Gilad, S., Meiri, E., Yogev, Y., Benjamin, S., Lebanony, D., Yerushalmi, N., Benjamin, H., Kushnir, M., Cholakh, H., Melamed, N., Bentwich, Z., Hod, M., Goren, Y., Chajut, A., 2008. Serum microRNAs are promising novel biomarkers. PLoS One 3, e3148.
Gupta, S., Read, D.E., Deepti, A., Cawley, K., Gupta, A., Oommen, D., Verfaillie, T., Matus, S., Smith, M.A., Mott, J.L., Agostinis, P., Hetz, C., Samali, A., 2012. Perk-dependent repression of miR-106b-25 cluster is required for ER stress-induced apoptosis. Cell. Death Dis. 3, e333.
Gurney, M.E., Pu, H., Chiu, A.Y., Dal Canto, M.C., Polchow, C.Y., Alexander, D.D., Caliendo, J., Hentati, A., Kwon, Y.W., Deng, H.X., 1994. Motor neuron degeneration in mice that express a human Cu, Zn superoxide dismutase mutation. Science 264, 1772–1775.
Haramati, S., Chapnik, E., Sztainberg, Y., Eilam, R., Zwang, R., Gershoni, N., McGlinn, E., Heiser, P.W., Wills, A.-M., Wirguin, I., Rubin, L.L., Misawa, H., Tabin, C.J., Brown, R., Chen, A., Hornstein, E., 2010. miRNA malfunction causes spinal motor neuron disease. Proc. Natl. Acad. Sci. U. S. A. 107, 13111–13116.
Hegedus, J., Putman, C.T., Tyreman, N., Gordon, T., 2008. Preferential motor unit loss in the SOD1 G93A transgenic mouse model of amyotrophic lateral sclerosis. J. Physiol. 586, 3337–3351.
Herdewyn, S., Cirillo, C., Van Den Bosch, L., Robberecht, W., Vanden Berghe, P., Van Damme, P., 2014. Prevention of intestinal obstruction reveals progressive neurodegeneration in mutant TDP-43 (A315T) mice. Mol. Neurodegener. 9, 24.
Hetz, C., Mollereau, B., 2014. Disturbance of endoplasmic reticulum proteostasis in neurodegenerative diseases. Nat. Rev. Neurosci. 15, 233–249.
Himanen, J.P., Chumley, M.J., Lackmann, M., Li, C., Barton, W.A., Jeffrey, P.D., Vearing, C., Geleick, D., Feldheim, D.A., Boyd, A.W., Henkemeyer, M., Nikolov, D.B., 2004. Repelling class discrimination: ephrin-A5 binds to and activates EphB2 receptor signaling. Nat. Neurosci. 7, 501–509.
Hovden, H., Frederiksen, J.L., Pedersen, S.W., 2013. Immune system alterations in amyotrophic lateral sclerosis. Acta Neurol. Scand. 128, 287–296.
Ittner, L.M., Halliday, G.M., Kril, J.J., Götz, J., Hodges, J.R., Kiernan, M.C., 2015. FTD and ALS-translating mouse studies into clinical trials. Nat. Rev. Neurol. 11, 360–366.
Jacquier, A., 2009. The complex eukaryotic transcriptome: unexpected pervasive transcription and novel small RNAs. Nat. Rev. Genet. 10, 833–844.
Jalali, S., Gandhi, S., Scaria, V., 2016. Navigating the dynamic landscape of long noncoding RNA and protein-coding gene annotations in GENCODE. Hum. Genomics 10, 35.
Janssens, J., Van Broeckhoven, C., 2013. Pathological mechanisms underlying TDP-43 driven neurodegeneration in FTLD-ALS spectrum disorders. Hum. Mol. Genet. 22, R77–R87.
Junker, A., Krumbholz, M., Eisele, S., Mohan, H., Augstein, F., Bittner, R., Lassmann, H., Wekerle, H., Hohlfeld, R., Meinl, E., 2009. MicroRNA profiling of multiple sclerosis lesions identifies modulators of the regulatory protein CD47. Brain 132, 3342–3352.
Katayama, Y., Maeda, M., Miyaguchi, K., Nemoto, S., Yasen, M., Tanaka, S., Mizushima, H., Fukuoka, Y., Arii, S., Tanaka, H., 2012. Identification of pathogenesis-related microRNAs in hepatocellular carcinoma by expression profiling. Oncol. Lett. 4, 817–823.
Kawahara, Y., Mieda-Sato, A., 2012. TDP-43 promotes microRNA biogenesis as a component of the Drosha and Dicer complexes. Proc. Natl. Acad. Sci. U. S. A. 109, 3347–3352.
Keller, A., Leidinger, P., Lange, J., Borries, A., Schroers, H., Scheffler, M., Lenhof, H.-P., Ruprecht, K., Meese, E., 2009. Multiple sclerosis: microRNA expression profiles accurately differentiate patients with relapsing-remitting disease from healthy controls. PLoS One 4, e7440.
Kiernan, M.C., Vucic, S., Cheah, B.C., Turner, M.R., Eisen, A., Hardiman, O., Burrell, J.R., Zoing, M.C., 2011. Amyotrophic lateral sclerosis. Lancet 377, 942–955.
Kimura, F., Fujimura, C., Ishida, S., Nakajima, H., Furutama, D., Uehara, H., Shinoda, K., Sugino, M., Hanafusa, T., 2006. Progression rate of ALSFRS-R at time of diagnosis predicts survival time in ALS. Neurology 66, 265–267.
Kin, T., Yamada, K., Terai, G., Okida, H., Yoshinari, Y., Ono, Y., Kojima, A., Kimura, Y., Komori, T., Asai, K., 2007. fRNAdb: a platform for mining/annotating functional RNA candidates from non-coding RNA sequences. Nucleic Acids Res. 35, D145–D148.
Kolde, G., Bachus, R., Ludolph, A.C., 1996. Skin involvement in amyotrophic lateral sclerosis. Lancet 347, 1226–1227.
Koval, E.D., Shaner, C., Zhang, P., du Maine, X., Fischer, K., Tay, J., Chau, B.N., Wu, G.F., Miller, T.M., 2013. Method for widespread microRNA-155 inhibition prolongs survival in ALS-model mice. Hum. Mol. Genet. 22, 4127–4135.
Kozomara, A., Griffiths-Jones, S., 2014. miRBase: annotating high confidence microRNAs using deep sequencing data. Nucleic Acids Res. 42, D68–D73.
Kumar, P., Dezso, Z., MacKenzie, C., Oestreicher, J., Agoulnik, S., Byrne, M., Bernier, F., Yanagimachi, M., Aoshima, K., Oda, Y., 2013. Circulating miRNA biomarkers for Alzheimer's disease. PLoS One 8, e69807.
Langmead, B., 2010. Aligning short sequencing reads with Bowtie. Curr. Protoc. Bioinformatics. Chapter 11, Unit 11.7.
Le Carré, J., Lamon, S., Léger, B., 2014. Validation of a multiplex reverse transcription and pre-amplification method using TaqMan(®) MicroRNA assays. Front. Genet. 5, 413.
Leblond, C.S., Kaneb, H.M., Dion, P.A., Rouleau, G.A., 2014. Dissection of genetic factors associated with amyotrophic lateral sclerosis. Exp. Neurol. 262, 91–101.
Lee, Y.S., Shibata, Y., Malhotra, A., Dutta, A., 2009. A novel class of small RNAs: tRNA-derived RNA fragments (tRFs). Genes Dev. 23, 2639–2649.

Lesko, L.J., Atkinson, A.J., 2001. Use of biomarkers and surrogate endpoints in drug development and regulatory decision making: criteria, validation, strategies, Annu. Rev. Pharmacol. Toxicol 41, 347–366.
Makino, K., Jinnin, M., Kajihara, I., Honda, N., Sakai, K., Masuguchi, S., Fukushima, S., Inoue, Y., Ihn, H., 2012. Circulating miR-142-3p levels in patients with systemic sclerosis. Clin. Exp. Dermatol. 37, 34–39.
Marcel, M., 2011. Cutadapt removes adapter sequences from high-throughput sequencing reads. EMBnet.journal Bioinforma. Action 17, 1.
Matus, S., Lopez, E., Valenzuela, V., Nassif, M., Hetz, C., 2013. Functional contribution of the transcription factor ATF4 to the pathogenesis of amyotrophic lateral sclerosis. PLoS One 8, e66672.
Medical Research Council, 1976. Aid to the Examination of the Peripheral Nervous System. Her Majesty's Stationary Office; Medical Research Council, London.
Medinas, D.B., Valenzuela, V., Hetz, C., 2017. Proteostasis disturbance in amyotrophic lateral sclerosis. Hum. Mol. Genet. 26, R91–R104.
Moloney, E.B., de Winter, F., Verhaagen, J., 2014. ALS as a distal axonopathy: molecular mechanisms affecting neuromuscular junction stability in the presymptomatic stages of the disease. Front. Neurosci. 8, 252.
Morlando, M., Dini Modigliani, S., Torrelli, G., Rosa, A., Di Carlo, V., Caffarelli, E., Bozzoni, I., 2012. FUS stimulates microRNA biogenesis by facilitating co-transcriptional Drosha recruitment. EMBO J. 31, 4502–4510.
Naqvi, A.R., Fordham, J.B., Nares, S., 2015. miR-24, miR-30b, and miR-142-3p regulate phagocytosis in myeloid inflammatory cells. J. Immunol. 194, 1916–1927.
Nassif, M., Valenzuela, V., Rojas-Rivera, D., Vidal, R., Matus, S., Castillo, K., Fuentealba, Y., Kroemer, G., Levine, B., Hetz, C., 2014. Pathogenic role of BECN1/Beclin 1 in the development of amyotrophic lateral sclerosis. Autophagy 10, 1256–1271.
Neumann, M., Sampathu, D.M., Kwong, L.K., Truax, A.C., Micsenyi, M.C., Chou, T.T., Bruce, J., Schuck, T., Grossman, M., Clark, C.M., McCluskey, L.F., Miller, B.L., Masliah, E., Mackenzie, I.R., Feldman, H., Feiden, W., Kretzschmar, H.A., Trojanowski, J.Q., Lee, V.M.-Y., 2006. Ubiquitinated TDP-43 in frontotemporal lobar degeneration and amyotrophic lateral sclerosis. Science 314, 130–133.
Nicolas, F.E., Lopez-Martinez, A.F., 2010. MicroRNAs in human diseases. Recent Pat. DNA Gene Seq. 4, 142–154.
Nzwalo, H., de Abreu, D., Swash, M., Pinto, S., de Carvalho, M., 2014. Delayed diagnosis in ALS: the problem continues. J. Neurol. Sci. 343, 173–175.
Okumura, T., Shimada, Y., Omura, T., Hirano, K., Nagata, T., Tsukada, K., 2015. MicroRNA profiles to predict postoperative prognosis in patients with small cell carcinoma of the esophagus. Anticancer Res. 35, 719–727.
Ortega, F.J., Mercader, J.M., Moreno-Navarrete, J.M., Rovira, O., Guerra, E., Esteve, E., Xifra, G., Martínez, C., Ricart, W., Rieusset, J., Rome, S., Karczewska-Kupczewska, M., Straczkowski, M., Fernández-Real, J.M., 2014. Profiling of circulating microRNAs reveals common microRNAs linked to type 2 diabetes that change with insulin sensitization. Diabetes Care 37, 1375–1383.
Paez-Colasante, X., Figueroa-Romero, C., Sakowski, S.A., Goutman, S.A., Feldman, E.L., 2015. Amyotrophic lateral sclerosis: mechanisms and therapeutics in the epigenomic era. Nat. Rev. Neurol. 11, 266–279.
Paixão, S., Balijepalli, A., Serradj, N., Niu, J., Luo, W., Martin, J.H., Klein, R., 2013. EphrinB3/EphA4-mediated guidance of ascending and descending spinal tracts. Neuron 80, 1407–1420.
Parisi, C., Napoli, G., Amadio, S., Spalloni, A., Apolloni, S., Longone, P., Volonté, C., 2016. MicroRNA-125b regulates microglia activation and motor neuron death in ALS. Cell Death Differ. 23, 531–541.
Patel, R.K., Jain, M., 2012. NGS QC Toolkit: a toolkit for quality control of next generation sequencing data. PLoS One 7, e30619.
Peters, O.M., Ghasemi, M., Brown, R.H., 2015. Emerging mechanisms of molecular pathology in ALS. J. Clin. Invest. 125, 1767–1779.
Pivarcsi, A., Meisgen, F., Xu, N., Ståhle, M., Sonkoly, E., 2013. Changes in the level of serum microRNAs in patients with psoriasis after antitumour necrosis factor-α therapy. Br. J. Dermatol. 169, 563–570.
Polymenidou, M., Lagier-Tourenne, C., Hutt, K.R., Huelga, S.C., Moran, J., Liang, T.Y., Ling, S.-C., Sun, E., Wancewicz, E., Mazur, C., Kordasiewicz, H., Sedaghat, Y., Donohue, J.P., Shiue, L., Bennett, C.F., Yeo, G.W., Cleveland, D.W., 2011. Long pre-mRNA depletion and RNA missplicing contribute to neuronal vulnerability from loss of TDP-43. Nat. Neurosci. 14, 459–468.
Renton, A.E., Chiò, A., Traynor, B.J., 2014. State of play in amyotrophic lateral sclerosis genetics. Nat. Neurosci. 17, 17–23.
Rhead, B., Karolchik, D., Kuhn, R.M., Hinrichs, A.S., Zweig, A.S., Fujita, P.A., Diekhans, M., Smith, K.E., Rosenbloom, K.R., Raney, B.J., Pohl, A., Pheasant, M., Meyer, L.R., Learned, K., Hsu, F., Hillman-Jackson, J., Harte, R.A., Giardine, B., Dreszer, T.R., Clawson, H., Barber, G.P., Haussler, D., Kent, W.J., 2010. The UCSC genome Browser database: update 2010. Nucleic Acids Res. 38, D613–D619.
Schöler, N., Langer, C., Döhner, H., Buske, C., Kuchenbauer, F., 2010. Serum microRNAs as a novel class of biomarkers: a comprehensive review of the literature. Exp. Hematol. 38, 1126–1130.
Shao, N.-Y., Hu, H.Y., Yan, Z., Xu, Y., Hu, H., Menzel, C., Li, N., Chen, W., Khaitovich, P., 2010. Comprehensive survey of human brain microRNA by deep sequencing. BMC Genomics 11, 409.
Shioya, M., Obayashi, S., Tabunoki, H., Arima, K., Saito, Y., Ishida, T., Satoh, J., 2010. Aberrant microRNA expression in the brains of neurodegenerative diseases: miR-29a decreased in Alzheimer disease brains targets neurone navigator 3. Neuropathol. Appl. Neurobiol. 36, 320–330.
Shrestha, A., Carraro, G., El Agha, E., Mukhametshina, R., Chao, C.-M., Rizvanov, A., Barreto, G., Bellusci, S., 2015. Generation and Validation of miR-142 Knock Out Mice. PLoS One 10, e0136913.
Sreedharan, J., Brown, R.H., 2013. Amyotrophic lateral sclerosis: problems and prospects. Ann. Neurol. 74, 309–316.
Takahashi, I., Hama, Y., Matsushima, M., Hirotani, M., Kano, T., Hohzen, H., Yabe, I., Utsumi, J., Sasaki, H., 2015. Identification of plasma microRNAs as a biomarker of sporadic Amyotrophic Lateral Sclerosis. Mol. Brain 8, 67.
Taylor, J.P., Brown, R.H., Cleveland, D.W., 2016. Decoding ALS: from genes to mechanism. Nature 539, 197–206.
Toivonen, J.M., Manzano, R., Oliván, S., Zaragoza, P., García-Redondo, A., Osta, R., 2014. MicroRNA-206: a potential circulating biomarker candidate for amyotrophic lateral sclerosis. PLoS One 9, e89065.
Traynor, B.J., Codd, M.B., Corr, B., Forde, C., Frost, E., Hardiman, O.M., 2000. Clinical features of amyotrophic lateral sclerosis according to the El Escorial and Airlie House diagnostic criteria: a population-based study. Arch. Neurol. 57, 1171–1176.
Turner, M.R., Talbot, K., 2013. Mimics and chameleons in motor neurone disease. Pract. Neurol. 13, 153–164.
Turner, M.R., Kiernan, M.C., Leigh, P.N., Talbot, K., 2009. Biomarkers in amyotrophic lateral sclerosis. Lancet Neurol. 8, 94–109.
Turner, M.R., Bowser, R., Bruijn, L., Dupuis, L., Ludolph, A., McGrath, M., Manfredi, G., Maragakis, N., Miller, R.G., Pullman, S.L., Rutkove, S.B., Shaw, P.J., Shefner, J., Fischbeck, K.H., 2013a. Mechanisms, models and biomarkers in amyotrophic lateral sclerosis. Amyotroph. Lateral Scler. Frontotemporal Degener. 14 Suppl 1, 19–32.
Turner, M.R., Hardiman, O., Benatar, M., Brooks, B.R., Chio, A., de Carvalho, M., Ince, P.G., Lin, C., Miller, R.G., Mitsumoto, H., Nicholson, G., Ravits, J., Shaw, P.J., Swash, M., Talbot, K., Traynor, B.J., Van den Berg, L.H., Veldink, J.H., Vucic, S., Kiernan, M.C., 2013b. Controversies and priorities in amyotrophic lateral sclerosis. Lancet Neurol. 12, 310–322.
Van Goethem, A., Yigit, N., Everaert, C., Moreno-Smith, M., Mus, L.M., Barbieri, E., Speleman, F., Mestdagh, P., Shohet, J., Van Maerken, T., Vandesompele, J., 2016. Depletion of tRNA-halves enables effective small RNA sequencing of low-input murine serum samples. Sci. Rep. 6, 37876.
Van Hoecke, A., Schoonaert, L., Lemmens, R., Timmers, M., Staats, K.A., Laird, A.S., Peeters, E., Philips, T., Goris, A., Dubois, B., Andersen, P.M., Al-Chalabi, A., Thijs, V., Turnley, A.M., van Vught, P.W., Veldink, J.H., Hardiman, O., Van Den Bosch, L., Gonzalez-Perez, P., Van Damme, P., Brown, R.H., van den Berg, L.H., Robberecht, W., 2012. EPHA4 is a disease modifier of amyotrophic lateral sclerosis in animal models and in humans. Nat. Med. 18, 1418–1422.
van Zundert, B., Brown, R.H., 2016. Silencing strategies for therapy of SOD1-mediated ALS. Neurosci. Lett. 636, 32–39.
van Zundert, B., Peuscher, M.H., Hynynen, M., Chen, A., Neve, R.L., Brown, R.H., Constantine-Paton, M., Bellingham, M.C., 2008. Neonatal neuronal circuitry shows hyperexcitable disturbance in a mouse model of the adult-onset neurodegenerative disease amyotrophic lateral sclerosis. J. Neurosci. 28, 10864–10874.
Victoria, B., Dhahbi, J.M., Nunez Lopez, Y.O., Spinel, L., Atamna, H., Spindler, S.R., Masternak, M.M., 2015. Circulating microRNA signature of genotype-by-age interactions in the long-lived Ames dwarf mouse. Aging Cell 14, 1055–1066.
Wegorzewska, I., Bell, S., Cairns, N.J., Miller, T.M., Baloh, R.H., 2009. TDP-43 mutant transgenic mice develop features of ALS and frontotemporal lobar degeneration. Proc. Natl. Acad. Sci. U. S. A. 106, 18809–18814.
Williams, A.H., Valdez, G., Moresi, V., Qi, X., McAnally, J., Elliott, J.L., Bassel-Duby, R., Sanes, J.R., Olson, E.N., 2009. MicroRNA-206 delays ALS progression and promotes regeneration of neuromuscular synapses in mice. Science 326, 1549–1554.
Wu, H., Neilson, J.R., Kumar, P., Manocha, M., Shankar, P., Sharp, P.A., Manjunath, N., 2007. miRNA profiling of naïve, effector and Memory CD8 T cells. PLoS One 2, e1020.
Xie, C., Yuan, J., Li, H., Li, M., Zhao, G., Bu, D., Zhu, W., Wu, W., Chen, R., Zhao, Y., 2014. NONCODEv4: exploring the world of long non-coding RNA genes. Nucleic Acids Res. 42, D98–D103.
Yan, S., Wang, T., Huang, S., Di, Y., Huang, Y., Liu, X., Luo, Z., Han, W., An, B., 2016. Differential expression of microRNAs in plasma of patients with prediabetes and newly diagnosed type 2 diabetes. Acta Diabetol. 53, 693–702.
Zhao, W., Beers, D.R., Henkel, J.S., Zhang, W., Urushitani, M., Julien, J.P., Appel, S.H., 2010. Extracellular mutant SOD1 induces microglial-mediated motoneuron injury. Glia 58, 231–243.
Zhong, X.Y., Holzgreve, W., Huang, D.J., 2008. Isolation of cell-free RNA from maternal plasma. Methods Mol. Biol. 444, 269–273.
Zhou, F., Guan, Y., Chen, Y., Zhang, C., Yu, L., Gao, H., Du, H., Liu, B., Wang, X., 2013. miRNA-9 expression is upregulated in the spinal cord of G93A-SOD1 transgenic mice. Int. J. Clin. Exp. Pathol. 6, 1826–1838.